FRUCTOSE ACTIVATES A STRESS RESPONSE SHARED BY METHYLGLYOXAL AND HYDROGEN PEROXIDE IN *STREPTOCOCCUS MUTANS*

Alejandro R. Walker, Danniel N. Pham, Payam Noeparvar, Alexandra M. Peterson, Marissa K. Lipp, José A. Lemos, and Lin Zeng[‡]

Department of Oral Biology, University of Florida College of Dentistry, Gainesville, Florida, USA.

Key words: Fructose, Methylglyoxal, Hydrogen Peroxide, F-1-P, Stress Response, Metal homeostasis, Gene Regulation.

[‡] Corresponding author:

Lin Zeng, PhD

1395 Center Drive

Gainesville, FL 32610

Email: lzeng@dental.ufl.edu

Phone: (352) 273-8868

Abstract

Fructose catabolism by *Streptococcus mutans* is initiated by three PTS transporters yielding fructose-1-phoshate (F-1-P) or fructose-6-phosphate. Deletion of one such F-1-P-generating PTS, *fruI*, was shown to reduce the cariogenicity of *S. mutans* in rats fed a high-sucrose diet. Moreover, a recent study linked fructose metabolism in *S. mutans* to a reactive electrophile species (RES) methylglyoxal. Here, we conducted a comparative transcriptomic analysis of *S. mutans* treated briefly with 50 mM fructose, 50 mM glucose, 5 mM methylglyoxal, or 0.5 mM hydrogen peroxide (H_2O_2). The results revealed a striking overlap between the fructose and methylglyoxal transcriptomes, totaling 176 genes, 61 of which were also shared with the H_2O_2 transcriptome. This core of 61 genes encompassed many of the same pathways affected by exposure to low pH or zinc intoxication. Consistent with these findings, fructose negatively impacted metal homeostasis of a mutant deficient in zinc expulsion and the growth of a mutant of the major oxidative stress regulator SpxA1. Importantly, fructose metabolism lowered culture pH at a faster pace, allowed better survival under acidic and nutrient-depleted conditions, and enhanced the competitiveness of *S. mutans* against *Streptococcus sanguinis*, although a moderated level of F-1-P might further boost some of these benefits. Conversely, several commensal streptococcal species displayed a greater sensitivity to fructose that may negatively affect their persistence and competitiveness in dental biofilm. In conclusion, fructose metabolism is integrated into the stress core of *S. mutans* and regulates critical functions required for survival and its ability to induce dysbiosis in the oral cavity.

Importance. Fructose is a common monosaccharide in the biosphere, yet its overconsumption has been linked to various health problems in humans including insulin resistance, obesity, diabetes, non-alcoholic liver diseases, and even cancer. These effects are in large part attributable to the unique biochemical characteristics and metabolic responses associated with the degradation of fructose. Yet, an understanding of the effects of fructose on the physiology of bacteria and its implications to the human microbiome is severely lacking. Here we performed a series of analyses on the gene regulation of a dental pathogen *Streptococcus mutans* by exposing it to fructose and other important stress agents. Further supported by growth, persistence, and competition assays, our findings revealed the ability of fructose to activate a set of stress-related functions that may prove critical to the ability of the bacterium to persist and cause diseases both within and without of the oral cavity.

Introduction

Disruption in microbial homeostasis in human microbiomes, a condition termed dysbiosis, has been associated with the development of many diseases that range from GI tract disorders such as inflammatory bowel disease and pseudomembranous colitis to oral infectious diseases such as dental caries, candidiasis, and periodontitis (1, 2). Carbohydrate metabolism plays a vital role in oral health by contributing to the biochemistry and ecology of oral microbiota. It is widely understood that overconsumption of refined carbohydrates is a defining factor in the development of dysbiosis through acid production and establishment of an acidogenic and aciduric dental biofilm (3-6). Emerging evidence also supports the co-occurrence of dental caries and periodontal diseases, pointing to potentially shared mechanisms in underlying etiology (7-9). With the food industry shifting heavily toward the use of fructose and fructose-releasing sugars in the past several decades and the concurrent pandemic of metabolic syndrome, the impact of dietary fructose to oral and systemic health demands urgent attention (10).

Fructose is a ubiquitous nutrient widely found in fruits, yet overconsumption of fructose is often associated with adverse health outcomes in humans that include insulin resistance, obesity, liver diseases, systemic inflammation, type-2 diabetes, cogitative decline, and even cancer (11-15). According to the “fructose survival hypothesis”, fructose triggers a conserved cellular response in mammalian cells that manifests as mitochondrial oxidative stress and reduced cellular ATP levels, accompanied by behavioral changes that includes hunger, thirst, foraging, and weight gain (16). While this response could have been limited and beneficial to animals and our

human ancestors, the negative effects of fructose have been greatly exacerbated by its widespread use in Western diet.

Streptococci are the most abundant commensal species colonizing oral surfaces, and most of them rely on carbohydrate fermentation, via the Embden–Meyerhof–Parnas (EMP) pathway of glycolysis, to produce energy and precursors for various biogenesis processes (3). Multiple fructose-transporting mechanisms exist in streptococci, each harboring a fructose: phosphotransferase (PTS) permease that generates either fructose-1-phosphate (F-1-P) or fructose-6-phosphate (F-6-P), which is further phosphorylated into F-1,6-bP by their respective phosphofructokinases (17). Studies so far have indicated that F-1-P metabolism contributes to *in vitro* fitness, biofilm development, and virulence for pathogenic species such as *Streptococcus pyogenes, Streptococcus agalactiae,* and *Streptococcus gordonii* (18-22). For the cariogenic pathobiont *Streptococcus mutans*, the primary fructose pathway is encoded by the *fruRKI* operon, encoding a negative regulator FruR, a PTS permease (FruI) that yields F-1-P, and a F-1-P kinase (FruK) (17). Deletion of *fruI* in *S. mutans* UA159 resulted in lower levels, though not complete lack of F-1-P when exposed to fructose (23) and reduced the ability of the bacterium to colonize and induce dentin caries in rats fed a high-sucrose diet (24). Based on genetic studies, expression of *fruRKI,* and its homologue *fruRBA* in related streptococci, is inducible by F-1-P which acts allosterically on FruR (17, 18, 25). Another fructose-PTS (EII^{Lev}), encoded by *levDEFG,* exists in some of these oral streptococci, including *S. mutans, Streptococcus sanguinis* and *S. gordonii*, which likely generates F-6-P and requires a four-component system LevQRST for induction in response to extracellular fructose (26). *S. mutans* harbors yet another

fructose-PTS (*fruCD*) that is also predicted to generate F-1-P, although its contribution to the overall fructose transport appears to be minor (17). Overall, the F-1-P pathway encoded by *fruRBA/fruRKI* operon is conserved in most Gram-positive bacteria encompassing *Bacillus, Enterococcus, Lactococcus, Lactobacillus, Clostridium, Listeria,* and most *Streptococcus* species (27-29). Moreover, *S. mutans, S. gordonii,* and *S. sanguinis* also harbor another fructose-related operon, *sppRA.* SppA has been characterized as a hexose-phosphate phosphohydrolase that specializes in dephosphorylating F-1-P, and F-6-P to a lesser extent; and SppR is a negative auto-regulator whose activity is allosterically regulated by F-1-P (23).

A recent study involving fructose centered on the molecular mechanisms required for oral streptococci to degrade a group of highly reactive electrophile species (RES), including methylglyoxal and glyoxal (30), which are created by all life as byproducts of glycolysis and serve as important immune effectors (31, 32). It has been reported that *S. mutans* is significantly more resistant to methylglyoxal than several commensal streptococci including *S. gordonii, S. sanguinis,* and members of the mitis group (30). A zinc-containing protein GloA2 (SMU.1112c), predicted to be a paralogue to the main methylglyoxal-degrading enzyme glyoxalase A (LguL or GloA) based on its sequence and crystal structure, was identified in all oral streptococci examined so far (30). The *gloA2*-null mutants of both *S. mutans* and *S. sanguinis* displayed increased chaining and autolysis upon treatment by fructose which resembled the effect of exposure to methylglyoxal, including its reversal by treatment with glutathione (GSH) which is known to scavenge methylglyoxal before degradation by LguL (32). Interestingly, the expression of *lguL* was inducible by growth on fructose, and the fructose-sensitivity of

gloA2 mutants was largely dependent on the integrity of the F-1-P-generating PTS, FruI (30). Herein we further examined fructose-dependent gene regulation and physiology in relation to streptococcal tolerance to important stressors including methylglyoxal and hydrogen peroxide. Our findings revealed the integration of fructose-mediated response with general stress response experienced during bacteria-host and inter-microbial interactions.

Results

Comparative RNA-seq analyses identified a stress core shared by methylglyoxal, fructose, and H_2O_2.

We previously performed an RNA-seq analysis on *S. mutans* cultured to the exponential phase with 0.5% fructose (27.7 mM) in the medium (33). The strain used in this study was a mutant deficient in several enzymes capable of degrading sucrose and other carbohydrate polymers (34), and was later revealed to contain a spontaneous mutation in a major peroxide-sensing regulator PerR (35). While this work provided us important information regarding the state of the bacterium after growing on fructose, these genetic deviations are of concern and the study could not capture the response the cells present immediately after fructose intake, as metabolic regulation tends to return to equilibrium after initial perturbance. To mimic the physiological impact to bacteria when humans consume a large dose of fructose in food or drinks, we cultured *S. mutans* strain UA159 (from ATCC) in a glucose-based medium to the exponential phase and then treated the cells with 50 mM fructose for 30 min, which were immediately processed for RNA-seq analysis in comparison to untreated controls.

Considering the similarity between glucose and fructose, the same UA159 cultures were treated with 50 mM glucose in the same manner and analyzed as an additional control. These concentrations of carbohydrates represent the physiological levels the microbiota likely encounter periodically in oral cavity. The experiment was also repeated using the same bacteria after treatment with 5 mM methylglyoxal for 30 min (30). In addition, we obtained and reanalyzed the datasets of a similar RNA-seq study performed on UA159 cultures that were prepared in a glucose-based medium and treated with 0.5 mM H_2O_2 for 5 min (36) (see Fig. 1 for volcano plots, Fig. 2 for Venn diagrams, Fig. S1 for principal component analyses, Fig. S2 for Gene Ontology term analyses, and supplemental Tables S1 to S3 for other details).

Methylglyoxal. Treatment of UA159 with 5 mM of methylglyoxal differentially affected the expression of a total of 474 genes when compared to the mock-treated control group, with 271 being up-regulated and 203 being down-regulated (Fig. 2, Fig. S2). Methylglyoxal is known to react with the reduced form of glutathione (GSH), which is interconnected with other reductive potentials such as NADPH and ascorbate (37). Treatment with methylglyoxal resulted primarily in several effects similar to oxidative stress response (36): increased expression of genes involved in thiol homeostasis including thioredoxins *trxAB*, GSH synthetase *gshAB* (38), glutathione reductase *gor,* and glutathione S-transferase *gst*; increased expression of the iron-sulfur (Fe-S) cluster biosynthesis system *sufCDSUB* (39), the ascorbate metabolic cluster (SMU.271 to SMU.275) (40), the reactive oxygen species (ROS) scavenging genes *sodA*, *ahpCF*, and *tpx*, and genes whose products are involved in metal homeostasis: copper exporter operon *copYAZ*, and iron-sequestering gene *dpr*. Also upregulated were several

transcription regulators known to be involved in stress management: *relS*, *perR*, *phoR/ycbL*, *scnKR*, *rcrRPQ*, SMU.1097c, *vicKX*, *comR*, *comDE*, and *lexA*. Likely as the need to restore the GSH/GSSG balance, treatment of methylglyoxal upregulated several putative aldo/keto reductases: SMU.382c and SMU.383c, SMU.677 to SMU.681, SMU.1040c, and SMU.1602 residing immediately upstream of *lguL* which encodes the major methylglyoxal-degrading enzyme LguL/GloA (both up by 3~4-fold). It is worth noting that most of these aldo/keto reductases, other than *lguL*, are absent in related commensal streptococci. Also related to improved reducing capacity was upregulation of several putative ribonucleotide reductases (41, 42): SMU.667 to SMU.669c, SMU.991, and SMU.2070 to SMU.2074 (*nrdG*).

Interestingly, methylglyoxal treatment reduced the expression of iron/manganese transporter *sloAB* (not *sloC*) and cognate *sloR* regulator. It also reduced the expression of ferrous ion transporter genes *feoAB*. These changes were consistent with the purported ability of GSH to buffer intracellular metal ions (43), as a release of these ions would likely increase the expression of metal exporters (*copYA*) but reduce that of metal importers (*sloABC* and *feoAB*). Another likely effect of methylglyoxal exposure is its reaction with intracellular amino acids such as arginine and lysine. For this, we observed increased expression of amino acid biosynthesis/transport operons, *argCJBD* for arginine and *livFGMHK* for branched-chain amino acids. As a general response to stressful stimuli, we observed elevated expression of genes required for DNA repair (*exoA*, *end3*, *mutY*, and *uvrA*) and protein or peptide degradation (*clpC, clpE, pepO*, and *pepP*). Conversely, there were also several stress management genes that showed reduced expression: *mreCD*, *irvR*, *hrcA, grpE,* and *dnaK*. Most ribosomal proteins and

the translation initiation factor InfC also had lower mRNA levels, indicative of reduced protein synthesis activity. There was likely a shift toward a more efficient, mixed-acid fermentation as we saw greater expression by acetoin metabolic operon (*adhABCD-lplA*), the related alpha-acetolactate metabolic genes *alsS* and *aldB*, NADH oxidase (*nox*), and a pyruvate-formate lyase activating enzyme *pflA*. At the same time, the genes encoding the two major enzymes of the PTS, *ptsH* and *ptsI*, along with the transport and metabolic pathways for mannitol (EII^{Mtl}, SMU.1184c and SMU.1185), cellobiose (EII^{Cel}, SMU.1596 to SMU.1600), sucrose (EII^{Scr}, SMU.1841 to SMU.1844), and glucose (EII^{Man}, SMU.1877 to SMU.1879) all showed significantly reduced expression.

Comparative analysis of methylglyoxal regulon with H_2O_2-mediated stress response. During the analysis of the methylglyoxal-induced transcriptomic shift, it was immediately apparent that many of these genes were also identified by a previous study on peroxide stress response of *S. mutans* UA159 (36). A closer inspection of the peroxide stress transcriptome identified a total of 115 genes (Supplemental Tables S1 and S4, Fig. 2A) as being shared by methylglyoxal and H_2O_2, indicative of the common bacterial mechanisms needed to deal with these two stressors. These aforementioned functions included ROS scavenging, thiol and metal homeostasis, DNA repair and protein processing, and energy metabolism. Out of these 115 genes, 100 showed upregulation and 12 were downregulated; only 3 showed different polarity of change. Important distinctions were also noted which encompassed 359 methylglyoxal-specific genes that were missing in H_2O_2 regulon, and conversely 79 H_2O_2-responsive genes absent in the

methylglyoxal regulon (Supplemental Table S4). Briefly, absent in H_2O_2-induced response included the reduced expression of the PTS genes, namely *ptsH, ptsI*, and EII^{Mtl}, EII^{Cel}, EII^{Scr}, and EII^{Man} operons. Also absent were genes for ribosomal proteins, *lrgAB-lytST*, *argCJBD* and agmatine deiminase operon (44), several putative aldo/keto reductase clusters, potassium transporters *trkAB*, the *nrd* operon SMU.2070 to SMU.2074, *mreCD*, *hrcA-grpE-dnaK*, and transcription regulators including *mleR, relS*, *phoR/ycbL*, *nagR*, *irvR, vicKX, comX,* and *ahrC*. Missing from the methylglyoxal regulon were some of the H_2O_2-induced genes, including mutacin genes (*nlmABCD* and *nlmTE*), *sloC*, *liaSR, levQRST, relA,* and the zinc import operon *adcBCR.* Interestingly, while methylglyoxal induced expression of most of the competence regulators, *comCDE, comR*, and *rcrR* (45), and the late-competence operon *comYA-YI* (46), H_2O_2 reduced expression of two important *nlm* operons, one of which (*nlmABCD*) requires an active *comDE* circuit for expression (47).

Significant overlap between fructose, methylglyoxal, and H_2O_2-mediated responses. Treatment of UA159 with 50 mM fructose for 30 min differentially affected the expression of a total of 449 genes, with 250 being up-regulated and 199 being down-regulated (Fig. 2B, Fig. S2, and Table S3). Though not a critical point of this study, these findings represent a striking difference in gene regulation compared to what was previously observed in UA159 grown with 0.5% fructose (33). As a control, similar treatment with 50 mM glucose for 30 min also upregulated 128 genes and down-regulated 216 genes (Table S3). Significantly, there was a larger overlap between the genes affected by fructose and methylglyoxal, totaling 176 genes (98 up and 62 down,

16 with opposite directions of change), compared to the 116-gene overlap between glucose and methylglyoxal (38 up and 48 down, 30 with opposite directions of change). Among the 176 genes shared by methylglyoxal and fructose, 61 overlapped the H_2O_2 regulon; among the 116 genes shared by methylglyoxal and glucose, only 24 overlapped with the H_2O_2 regulon (Table S5). Therefore, compared to glucose, significantly more genes were shared by treatment of fructose with that of methylglyoxal and H_2O_2. Comparative analysis identified a set of 44 genes that were similarly affected by fructose, methylglyoxal, and H_2O_2, excluding 17 genes impacted by all four treatments. Altogether, these 61 genes (Table S5 tab "Core genes") encoded for some of the aforementioned functions such as thiol and metal homeostasis (*trxAB, gst, gor, sloA, dpr,* and *sufCDSUB*,), enzymes for ROS scavenging (*sodA, ahpCF,* and *tpx*) and restoration of redox balance (*nox*, ascorbate operon, *gapN*, and multiple *nrd* genes), glucan-binding protein *gbpC*, proteins implicated in general stress management including *clpE, clpL*, *uvrA, mutY,* SMU.503c (48), *exoA, lexA* (49), *pepP,* and *pepO* (50, 51), and transcription regulators such as *scnKR*, *perR,* and *msmR.* Again, nearly all 61 genes (except for 2) showed the same polarity of change under three treatments. Notably, many genes shared by glucose and fructose, e.g., *sloA, sodA, gor, tpx, gst, trxAB*, and *lexA*, showed significantly greater change due to the treatment by fructose than by glucose of the same amount.

Also included in this group of genes was the CRISPR1-Cas system (SMU.1402c to SMU.1406c) that was repressed by all four treatments, although the effect of H_2O_2 was slightly below the 2-fold threshold (Table S1). Conversely affected was the 10-gene CRISPR2-Cas cluster (SMU.1753c to SMU.1764c) that produced increased levels of

transcripts under all four conditions, despite that the induction of several genes by methylglyoxal or glucose was below the threshold. An earlier study characterizing these two systems in *S. mutans* suggested that CRISPR-Cas overall was required for tolerance towards membrane, thermal, pH, and oxidative stressors (52). The differential regulation of these two systems in response to carbohydrates, methylglyoxal, and H_2O_2 warrants further exploration. It is also worth noting that the relative impact of fructose to both clusters was the highest among all four treatments.

<u>*Similarity between responses to fructose and glucose*</u>. Considering the effects of carbohydrates in increasing osmolarity and acid production, it was not surprising to find a substantial overlap between fructose- and glucose-responsive genes (total 165 genes, 80 genes when excluding methylglyoxal and H_2O_2; Supplemental Table S6), although many (near 50%) encoded hypothetical proteins. Interestingly, the operon required for malolactic fermentation (SMU.137-SMU.141) were most highly induced by either treatment, with the mRNA levels increasing by 12~20-fold. Considering the inducibility of this system by acidic pH (53, 54), a rapid drop in pH due to glycolytic activities likely triggered this response. The agmatine deiminase (*aguA*) that has been shown to contribute to acid tolerance through production of ammonia (44) was similarly upregulated. Also induced by both carbohydrates were the majority of the genes/ORFs included in the genomic island TnSmu1 (55), from SMU.196c to SMU.215c, showing an increase in expression by 2~4-fold. Other notably upregulated genes included the SMU.1602/*lguL* cluster, the zinc/cadmium-exporter *zccE* (56), the glucosyltransferase *gtfD*, the fructosyltransferase *ftf*, a putative F-1-P kinase *pfk* (17), the lactose operon

(57), and the HPr kinase/phosphatase *hprK*. The fact that SMU.1602/*lguL* cluster was induced by methylglyoxal, fructose, and glucose suggested that endogenous production of methylglyoxal or related RES likely increased because of rapid influx of carbohydrates. Like before, *zccE* expression was >2-fold higher when treated with fructose compared to treatment by glucose. One cluster, SMU.1903c to SMU.1913c, along with the orphan response regulator *gcrR* (58), showed reduced expression under both treatments.

<u>*Genes affected only by fructose.*</u> A total of 168 genes were differentially affected by fructose alone (Supplemental Table S6 tab "Fru only", Fig. S2A for enriched molecular functions). In addition to what have been discussed thus far, treatment with 50 mM fructose altered the expression of several pathways and additional genes required for carbohydrate metabolism. Namely, fructose upregulated the operons of *sppRA*, *fruRKI*, *levDEFG*, and the sorbitol PTS, however downregulated the nigerose PTS, the maltose PTS (*malT* or *ptsG*), *pfl,* the *msm* cluster (59), *galK*, *gtfC,* the glycogen operon (*glg*) (60), an α-glucan metabolic cluster (SMU.1564 to SMU.1571) (61), and importantly the fructose-bisphosphate aldolase (*fbaA*, down 2-fold) which is responsible for cleaving F-1,6-bP into dihydroxyacetone phosphate (DHAP) and glyceraldehyde 3-phosphate (GADP). Expression of three additional clusters was notably affected by fructose alone. First, SMU.1057 to SMU.1063, encoding SatCDE, Ffh, YlxM, and two ABC transporters, were upregulated by 2- to 3-fold. This cluster has been implicated in protein translocation and acid tolerance in *S. mutans* (62). Second, operon (SMU.1527 to SMU.1534) which encodes for the F_1F_0-ATPase complex were downregulated by 2- to

3-fold. It was reported that the F_1F_0-ATPase, whose main function in *S. mutans* is expelling excess proton to the environment, was upregulated in response to a shift from steady state at pH 7 to pH 5 as part of the acid tolerance response (ATR) (63-65). Despite the likelihood of an acidic stress under the treatment of both glucose and fructose, there was no significant impact by glucose to this operon, and the treatment of fructose resulted in a lower rather than higher expression of all 8 genes encoding the F_1F_0-ATPase. Last, SMU.1734 to SMU.1745c, encoding for the pathway for fatty acid biosynthesis and similarly involved in ATR, showed 2- to 3-fold reduction in expression when treated with 50 mM fructose. While this effect was largely consistent with previous findings made in *S. mutans* under a glucose shock at 200 mM (65), here again 50 mM glucose failed to induce a similar response. Considering the importance of both pathways in maintaining membrane integrity and overall fitness, these findings could provide explanations to previously reported fructose-specific phenotypes such as autolysis and increased biofilm development (23, 30).

RT-qPCR analysis. Detailed transcriptional analyses were carried out to validate and further understand these findings, focusing on a list of genes relevant to bacterial fitness and pathogenicity. Considering the dynamic nature of gene regulation, mRNA abundance was compared in *S. mutans* UA159 treated with 50 mM fructose or 0.5 mM H_2O_2, each for 5 min and 30 min. Also included were the original treatments (30 min) of 5 mM methylglyoxal and 50 mM glucose, as well as two control conditions of growth in FMC-glucose and FMC-fructose. As shown in Table 1, mRNA levels of these 20 genes in the 4 treatments used in RNA-seq study confirmed their respective impact, including

upregulation in functions such as radical scavenging, RES degradation, copper export, thiol homeostasis, and stress-responsive regulators; and downregulation of *mreC*, cellobiose PTS component *celB*, and mutacin gene *nlmA*. Thirty-min compared to 5-min treatment with H_2O_2 generally gave more substantial activation of most genes tested. Similarly, a time-dependent response to fructose was noted for genes *lguL*, *sloA*, *celB*, *lexA*, *gshAB,* and *sppA*, although several did show signs of reversal in impact, namely *scnK, gbpC, nrdG*, and SMU.667. To test the significance of F-1-P to gene regulation, a *fruI* null mutant was treated with 50 mM fructose for 30 min. To our surprise, only 4 out 16 tested genes showed a reversal in impact due to loss of FruI, suggesting that FruI-mediated effect plays only a partial role in the extensive transcriptomic reprogramming triggered by the fructose treatment.

Fructose impacts metal homeostasis and Spx-dependent oxidative stress response.

A likely effect of methylglyoxal on bacterial physiology was the reduction of intracellular GSH/GSSG ratio and potential impact on metal homeostasis. Previously it was demonstrated that a zinc/cadmium exporter ZccE was responsible for the high zinc tolerance of *S. mutans*, and its expression required a cognate regulator ZccR (56). Deletion of either *zccE* or *zccR* resulted in a peroxide sensitivity under high-zinc conditions due to a disturbed zinc/manganese ratio which could be alleviated by manganese supplementation. When we tested the growth phenotype of a *zccR* null mutant in TV medium (66), which contains ~19 μM of zinc according to ICP-OES analysis (56), the mutant nonetheless grew normally when supported by glucose as the

sole carbohydrate source (Fig. 3A). When fructose was substituted for glucose however, Δ*zccR* showed a significant reduction compared to the WT UA159 in both growth rate and the final optical density (Fig. 3B). Like reported before, addition of 25 μM $MnSO_4$ to the TV-fructose medium significantly alleviated the growth deficiency of Δ*zccR*. Importantly, after we introduced a *fruI* deletion into the *zccR* background, the double mutant grew at levels comparable to the WT UA159 on either glucose or fructose, without manganese supplementation (Fig. 3B). As *fruI* deletion was previously shown to reduce intracellular F-1-P levels (23), these findings strongly supported the theory that excess F-1-P levels negatively impacted metal homeostasis in *S. mutans*.

Since fructose-mediated transcriptome included a cohort of oxidative stress genes primarily regulated by SpxA1 (67), we repeated this growth assay by including a deletion mutant of *spxA1*. To our surprise, Δ*spxA1* grew at a faster rate in TV-fructose than in TV-glucose (Fig. 4A). Considering the relatively high zinc content in TV medium, we next switched to a chemically defined FMC medium that contained very little zinc but sufficient manganese (around 110 μM). In FMC medium, Δ*spxA1* grew relatively well on glucose but could not grow on fructose (Fig. 4B). When we introduced the same *fruI* deletion into the Δ*spxA1* background, the growth deficiency on fructose was greatly alleviated (Fig. 4C). At the same time, only modest benefit was observed on fructose when a *levD* deletion was introduced into Δ*spxA1.* Although the exact mechanisms remain to be clarified, the medium-specific fructose sensitivity of Δ*spxA1* added further support to the notion that F-1-P affects oxidative stress response and metal homeostasis by interacting with Spx-mediated regulation.

To further test this hypothesis, a P*sodA::gfp* promoter-reporter fusion was established in the WT UA159 background to assess the response of Spx-mediated regulation to the presence of fructose; the superoxide dismutase (*sodA*) requires Spx proteins for optimal expression (36). As shown in Fig. 5 and Fig. S3, the *sodA* promoter was activated by the presence of fructose in a dose-dependent manner, from levels as low as 0.5 mM, yet it only produced a modest and slightly delayed response to the presence of 0.5 mM of H_2O_2. While 0.5 mM H_2O_2 significantly impeded the growth of *S. mutans* [Fig. S4 and (68)], as much as 10 mM fructose showed little to now effect. To ascertain the nature of fructose-derived signal in this effect, *fruI* and *levD* deletions were each introduced into UA159 containing the P*sodA::gfp* fusion. Consistent with above observations, deletion of *fruI* but not *levD* resulted in the loss of fructose-dependent activation of the *sodA* promoter activity. As expected, deletion of *spxA1* also abolished the expression of *sodA* promoter (36). These results not only confirmed the role of F-1-P in influencing Spx regulation, but given the magnitude of impact, suggested that fructose may serve as a primary signal for bacterial response to environmental changes.

F-1-P is the likely allosteric inducer for activating the *fruRKI* operon. To assess the levels of fructose needed to induce the expression, we utilized a strain containing a promoter-reporter fusion P*fruR::cat* (20). Bacteria were cultured in glucose-based FMC medium and then exposed to different amounts of fructose for 30 min. CAT activities from UA159/P*fruR::cat* suggested that at levels as low as 20 μM, fructose can significantly induce the expression of the *fruRKI* operon (Table S7).

Fructose contributes to fitness during starvation, acidic pH, and competition with peroxigenic streptococci.

Our previous studies have suggested that fructose, when used in excess under laboratory conditions, may induce autolysis and cell death. Paradoxically, considering the activation of much of the stress response core by fructose, we could anticipate improved persistence under stressful conditions. To test this hypothesis, we subjected *S. mutans* to a series of physiological tests by exposing it to fructose. First, strain UA159 was cultivated in FMC with 20 mM glucose or fructose, and their CFU was monitored while these cultures were continuously incubated without medium refreshment for 11 days. While fructose produced lower CFU than glucose at day 1 of the incubation as reported previously (23), it maintained the CFU of UA159 by at least 1 log higher than on glucose throughout the rest of the experiment (Fig. 6A). When 1 mM fructose was used together with 19 mM glucose, the fructose-associated effects were reduced and limited to the first two days of the incubation. We then repeated this experiment using strain Δ*fruI* (Fig. 6B). Echoing the findings in RT-qPCR analysis, Δ*fruI* showed significantly higher persistence than the wild-type parent, especially when fructose was used.

As a further test of acid tolerance under the fructose condition, we cultured UA159 for 20 h in a TV medium (FMC contains 10 mM phosphate buffer thus not ideal) supported with different amounts of glucose or fructose and measured the resting pH of these cultures. The results (Table 2) showed comparable growth yield but significantly lower resting pH in TV-fructose cultures than in TV-glucose cultures. For comparison, we conducted the same experiment on a health-associated commensal, *S. sanguinis* (SSA)

strain SK36. To our surprise, SK36 failed to produce a substantial growth on fructose, especially for higher concentrations (100 or 200 mM). Similar findings were made when this experiment was repeated using another *S. sanguinis* isolate BCC23 (69). Further tests on a number of low-passage, clinical isolates of additional commensal streptococci (70), encompassing the species of *S. gordonii, S. mitis, S. oralis, S. dentisani, S. intermedius, S. sp.* A12*, S. parasanguinis,* and *S. cristatus*, showed similar sensitivity in most but not all species (e.g., *S. intermedius*) tested (Table 2). On the contrary, tests on 6 additional WT *S. mutans* strains (Table S8) indicated that most of them were able to grow comparably well on fructose, and lowered the environmental pH to similar levels to that achieved on glucose. However, one isolate, OMZ175 of serotype *f* known for its collagen-binding and invasive activities (71), did show a modest sensitivity to fructose by having lower final OD_{600} and notably higher resting pH on fructose than glucose. We then performed a pH drop assay to further test the notion that fructose could lower the culture pH better than glucose. When a suspension of UA159 cells from an exponential phase, fructose-grown culture was fed 50 mM of fructose without buffering, it lowered the environmental pH at a notably faster rate, which ended at a significantly lower point, than a glucose-grown culture of UA159 did in 50 mM glucose (Fig. 7A and Fig. S5). It appeared that *S. mutans* UA159 catabolized fructose more rapidly than glucose and was more acid-tolerant under fructose conditions. We also performed this assay using BHI-grown bacteria for pH drops with glucose or fructose, which showed a similar, albeit smaller difference between these two sugars. We conclude that while most *S. mutans* strains tested by us appear well adapted to fermenting fructose, *S. sanguinis* and many commensal streptococci may be less capable of tolerating high levels of fructose.

Next, *S. mutans* was subjected to a competition assay in a mixed-species planktonic culture with the peroxigenic commensal *S. sanguinis*. Cultures from the exponential phase were mixed at approximately 1:1 ratio between two species and diluted into the FMC medium supplemented with 20 mM of glucose or fructose. After an overnight of incubation, CFUs for each species were enumerated by plating on selective agar plates (Fig. S6 includes CFU from mixed-species cultures and single-species controls). The resultant competitive indices (Fig. 7B) indicated a greater competitiveness for *S. mutans* UA159 in the presence of fructose than glucose, especially when used at higher concentrations. It is perhaps worth noting that this competitiveness of UA159 favored by fructose was at least partly attributable to the fructose sensitivity of its competitor, SK36, a phenotype that could be species- and even strain-specific (Table 2). Interestingly, deleting *spxB* in SK36 did not significantly change the competitive indices (Fig. S6E, 20 mM carbohydrates) whereas deleting *fruI* in UA159 further enhanced the competitiveness of *S. mutans* against *S. sanguinis* SK36 when supported with fructose. Since Δ*fruI* has a defect in fructose transport and grows more slowly than the WT on fructose (17), these and earlier results (Fig. 6B) suggested that a certain optimal level of F-1-P could benefit *S. mutans* when competing against commensal species capable of producing inhibitory levels of H_2O_2.

Discussion

It is frequently observed in stress biology that different stressors result in overlapping responses in bacteria (72). As an oral bacterium, *S. mutans* is frequently subjected to environmental insults that include acidic pH, oxygen and H_2O_2, hyperosmolarity, thermal

467 fluctuation, metal ions, and nutrient starvation (73). In this study, we identified
468 methylglyoxal and fructose as two potential stress signals capable of inducing
469 streptococcal stress responses (Fig. 8). A stress core comprised of 61 genes were
470 shared by the regulons of fructose, methylglyoxal, and H_2O_2. This commonality in gene
471 regulation can be attributed to the overlapping effects exerted by these treatments. For
472 example, exposure to concentrated sugars likely leads to acidic stress, hyperosmolarity,
473 and increased RES production. Treatments by both RES and ROS are expected to
474 perturb intracellular redox pools that could in turn influence bacterial metal and thiol
475 homeostasis. Exposure to extreme pH, RES, and ROS can all lead to denaturation of
476 amino acids, proteins, lipids, and nucleic acids. Each of these outcomes likely activates
477 a central regulatory system to restore essential nutrients or repair damage. Not
478 surprisingly, 40 out of the 61 core stress genes (Table S5) have been previously
479 identified in *S. mutans* by an acid adaptation study in response to either a glucose
480 shock (200 mM) or a shift from neutral to acidic pH (65). Conversely, only 17 out of the
481 61 stress-related genes were affected by our treatment of 50 mM glucose. The
482 discrepancy between our study and earlier findings by others (65) is likely due to the
483 difference in sugar content and culture conditions, as 200 mM glucose and continuous
484 culturing were used before as opposed to 50 mM glucose and batch cultures herein.
485 Corroborating the transcriptomic overlap between fructose and acid tolerance,
486 phenotypic analyses suggested a superior ability for *S. mutans*, particularly certain
487 strains such as UA159, GS-5 and ST1 (Table S8), to lower environmental pH when
488 fructose was used as the supporting carbohydrate, especially at higher concentrations.
489 This ability to tolerate fructose appears to be limited or absent in many commensal

490 streptococcal species we have tested so far, with potential species and strain specificity,
491 which may have important implications to microbial ecology in oral biofilms.
492 Furthermore, several pathways triggered by hyperosmolarity in previously studies (74-
493 76), including genes *lguL, sodA, nox*, the *opcA* cluster (SMU.2116 to SMU.2119), the
494 *opu/ffh/sat* cluster, and potassium uptake mechanism *trkAB*, were also identified as part
495 of the fructose/methylglyoxal/H_2O_2 response core.
496 Theories established in mostly Gram-negative bacteria suggest that methylglyoxal
497 bypass, a function that converts DHAP into pyruvate via the activities of a methylglyoxal
498 synthase (*mgsA*), two glyoxalases (*gloAB*), and a D-lactate dehydrogenase (D-*ldh*),
499 serves an important function in modulating glycolysis under sugar excess and
500 phosphate limitation (32). Genes *mgsA* and D-*ldh* are absent in most lactic acid bacteria
501 (LAB) genomes (30). However, methylglyoxal and related RES can be produced from
502 DHAP spontaneously or from a variety of other mechanisms (77). The conservation of
503 glyoxalases in streptococci (78) and the transcriptomic overlap among fructose,
504 glucose, and methylglyoxal support the notion that methylglyoxal metabolism is an
505 integral part of bacterial physiology, and the sources of methylglyoxal could be both
506 endogenous and exogenous. This conclusion is consistent with an emerging theory in
507 bacterial pathophysiology termed the aldehyde hypothesis (79), where a group of
508 reactive metabolic intermediates (RES) from the host and pathogens may serve as
509 potential antimicrobial effectors. This theory has supports from studies on LAB
510 pathogens that engage host immunity, including *S. pyogenes* and *S. agalactiae*, which
511 required glyoxalases for fitness and virulence (31, 78). For oral streptococci, the effects
512 of fructose on methylglyoxal metabolism could involve several mechanisms. First,

multiple RES compounds can be generated during fructose metabolism, given the presence of three phosphorylation products, F-1-P, F-6-P, and F-1,6-bP. Glucose metabolism generates only F-6-P and F-1,6-bP. DHAP is a direct product of cleavage of F-1,6-bP; cleavage of F-1-P by an aldolase produces glyceraldehyde (GA) and DHAP; and similarly, cleavage of F-6-P yields G3P and dihydroxyacetone (DHA). These metabolites are either themselves RES, e.g., GA, or in the case of DHAP and DHA, can generate methylglyoxal due to a reaction that is spontaneous or enzymatic in nature (MgsA). Second, fructose degradation may be regulated differently than glucose degradation, which could affect the accumulation or degradation of metabolic intermediates that are precursors of RES. Rapid phosphorylation of fructose by fructokinase and the resultant drawdown of ATP is a major factor in fructose-dependent metabolic impact in mammalian cells (16). Although in bacteria, carbohydrates are phosphorylated by PTS at the expense of PEP instead of ATP, here we showed a notably faster rate of glycolysis by *S. mutans* UA159 degrading fructose than glucose. As a result, fructose influx may alter the metabolism of F-6-P and F-1,6-bP, impacting RES production and gene regulation even in Δ*fruI* background. For example, accumulation of F-6-P and its degradation into DHA (instead of phosphorylation into F-1,6-bP) could presumably be amplified during high-fructose treatment, especially if F-1,6-bP cleavage is impeded. In support of these reasonings, fructose transcriptome reported downregulation of the F-1,6-bP aldolase *fbaA* (by 2-fold), and many common genes shared by fructose and glucose treatments produced a greater amplitude of change under the fructose condition. As part of the effort to understand the genetic mechanisms of fructose-specific biology, we have identified a novel 5-gene cluster, well

conserved in *S. mutans* and most streptococci, which encodes a putative F-6-P aldolase and a glycerol dehydrogenase (80, 81). Products of these genes could contribute to metabolism of F-6-P and DHA, as suggested by a study in *Listeria innocua* (82); and their overexpression was recently implicated in the hypervirulent phenotypes of a dominant GAS variant in England (83). Moreover, most Gram-positive bacteria maintain a novel LguL paralog, GloA2, whose deletion in *S. mutans* resulted in a fructose-specific phenotype that resembled methylglyoxal exposure (30). Highly pertinent to our research, an earlier animal study demonstrated that high fructose corn syrup (HFCS, 45% glucose and 55% fructose), despite producing no glucans, can induce dental caries in a rat model as effectively as sucrose (84). Likewise, *in vitro* studies by others reported that HFCS induced greater demineralization of tooth enamel compared to a similar treatment by sucrose (85).

In addition to influencing RES metabolism, F-1-P homeostasis appears to be an essential physiological signal in most streptococci. The *fruRKI/fruRBA* operon required for catabolizing fructose via the F-1-P pathway is highly conserved in most Gram-positive bacteria. Several oral streptococci also harbor the *sppRA* operon for moderating the F-1-P levels (23). We previously showed that a *fruK* deficient strain accumulated significant levels of F-1-P even at the absence of fructose and was highly defective in growth on fructose, suggesting an endogenous source of F-1-P (e.g., dephosphorylation of F-1,6,-bP) and the need to keep its level within an optimal range (23). Notably, the *sppRA* promoter required higher levels of fructose (25 to 50 mM) for induction (23), suggesting that *sppRA* are expressed only when F-1-P is above a certain threshold to avoid futile cycling between F-1-P and fructose. Conversely, we have

determined herein that 0.5 mM fructose is capable of activating Spx-mediated regulation and as little as 20 μM of fructose efficiently induced the expression of the *fruRKI* operon. We also observed in *S. sanguinis* the induction of *fruRBA* expression by similar levels of fructose or 25% human sera (Table S7). It is worth noting that for diabetic or hyperglycemic individuals, blood fructose levels are often significantly elevated as a function of the polyol pathway (16), capable of activating the *fruRKI/fruRBA* pathway (86). These findings allow us to posit that fructose regulates streptococcal function at both high (mM) and low (μM) levels, with the former contributing to fitness during the feast-and-famine cycle of the oral cavity and the latter in human circulatory system. While we only showed that fructose can benefit *S. mutans* at mM concentrations, we have good reasons to speculate that a similar benefit applies under μM levels of fructose. Several studies have suggested that *fruRKI/fruRBA* genes are required for streptococcal virulence during extraoral infections (19, 22, 83), where only sub-mM fructose is available, although the mechanisms remain uncharacterized. We further posit that fructose may trigger a surveillance mechanism against host-derived ROS and RES molecules, which primes bacterial stress response and additional fructose-specific pathways (Fig 8). Aside from FruR, SppR, LevQRST, and LacR that were previously shown to be responsive to fructose, herein we identified several transcription regulators whose expression appeared uniquely responsive to fructose treatment, including *spxA2, glnR, hdrR,* and a two-component system *spaRK*. Targeting these regulators and F-1-P-specific metabolism, i.e., GloA2, could help us unravel the molecular mechanisms required for cells to optimize stress management in response to fructose. With many oral streptococci existing as dual-niche organisms and the widespread use of fructose in

food, this research has implications in both oral microbial homeostasis and systemic health.

Lastly, it is worth reiterating that a fructose-PTS mutant (*frul*) of *S. mutans* displayed reduced colonization and cariogenicity in an earlier rat study under high-sucrose condition (24). This study revealed an important connection between fructose and sucrose in *S. mutans* physiology, as sucrose metabolism releases significant quantities of fructose both intracellularly and extracellularly, the latter of which can be reinternalized by the PTS (33, 34, 87). While it is tempting to speculate that fructose released from sucrose might contribute to virulence of *S. mutans* and influence the persistence of certain commensal streptococci, more in-depth investigation is needed to fully understand the role of fructose in caries development and biofilm dysbiosis.

Concluding remarks. By establishing a stress regulon shared by fructose, methylglyoxal, and H_2O_2, our study revealed a unique identity of fructose in streptococcal physiology as a fermentable substrate, a stressor, and potentially an important environmental signal. Gene regulations associated with an F-1-P homeostasis contributed to bacterial fitness under stressful conditions, especially for the cariogenic pathobiont *S. mutans*. The overlapping nature of stress response in general also suggests that fructose metabolism may affect the overall resilience against other stressors such as acidic pH, ROS, RES, toxic metals, starvation, and hyperosmolarity; conditions to be expected in both oral cavity and the blood stream (Fig. 8). Considering the widespread conservation of some of these genetic features, most of the fructose-

mediated effects discussed here are likely applicable to other lactic acid bacteria which have high relevance in both oral and systemic health.

Materials and Methods

Bacterial strains and culture conditions. Brain heart infusion (BHI) medium (Difco Laboratories, Detroit, MI) was used to maintain *S. mutans* and other streptococcal strains (Table 3). Liquid BHI was used to prepare for starter cultures for most of the experiments. Antibiotics were used, only when necessary, at the following concentrations: kanamycin (Km) 1 mg/mL, erythromycin (Em) 10 µg/mL, and spectinomycin (Sp) 1 mg/mL. For cultures requiring specific carbohydrates, a semi-defined Tryptone-Vitamin (TV) medium (66) or a synthetic medium FMC (88) was used, each supplemented with specified carbohydrates. Selection between TV and FMC was made based on the requirements of each experiment. Specifically, FMC was selected as the base medium when certain carbohydrates were added at very low levels, 1 mM or lower, to avoid potential contaminations from ingredients of TV. Similarly, FMC was used in promoter reporter study to reduce background fluorescence. TV and FMC also contain significantly different buffering capacity and levels of nutritional and toxic metal ions. Other than growth curves, all cultures were incubated without agitation at 37˚C in an aerobic atmosphere supplemented with 5% of CO_2.

For growth curves, bacterial cultures were diluted 100-fold into a TV or FMC medium containing specified carbohydrates, overlaid with 70 µL mineral oil, and maintained at 37˚C in a Bioscreen C lab system (Labsystems Oy, Helsinki, Finland) that recorded the optical density of the cultures at 600 nm (OD_{600}) every hour. A brief lateral shaking was

included before each reading to disperse aggregates. To monitor the expression levels of the *sodA* promoter over time using a P*sodA::gfp* reporter fusion, bacterial cultures from the exponential phase were similarly diluted into an FMC medium containing specified amounts of carbohydrates and H_2O_2 and overlaid with mineral oil. For 20 h, the OD_{600} and the relative fluorescence units (RFU) of the cultures (excitation 485/20 nm, emission 528/20 nm) were recorded hourly using a Synergy 2 Multi-Mode reader (BioTek, Winooski, VT). The RFU results were subtracted with the RFU readings from a control strain, which was of the same genetic background but without the *gfp* promoter fusion, before normalization against the corresponding OD_{600} of the culture (89).

Construction of genetic mutants. Genetic mutants of *S. mutans* were constructed through allelic exchange strategy and natural transformation facilitated by the use of competence-stimulating peptide (30). Recombinant DNA fragments used in this study were generated by PCR amplification and ligated together with antibiotic cassettes via Gibson Assembly (23). Primers used in DNA amplification and RT-qPCR are listed in Table S9. All mutants used in this study have been validated by PCR followed by Sanger sequencing. Promoter: reporter fusions were constructed using the plasmid pMC340B by inserting a promoter of interest in front of a promoterless *gfp* (green fluorescent protein) or *cat* (chloramphenicol acetyltransferase) gene, followed by integration at a distal site (between *mtlA* and *phnA*) of the chromosome unrelated to functions studied here (20).

RNA deep sequencing, transcriptomic analysis, and reverse transcriptase quantitative PCR (RT-qPCR). To compare bacterial gene regulation in response to fructose metabolism and exposure to methylglyoxal, *S. mutans* strain UA159 was cultivated to early exponential phase (OD_{600} = 0.4) in a chemically defined medium FMC (88) supplemented with 20 mM glucose. Bacteria were harvested by centrifugation (3,800× *g*, room temperature, 10 min), resuspended in fresh FMC containing 50 mM fructose, 50 mM glucose, or 5 mM methylglyoxal. An equal portion of the culture was kept in the original FMC-glucose medium as control. All samples were returned to incubation for 30 min before being harvested for RNA extraction.

RNA extraction and deep sequencing were carried out by following a previously published protocol detailed elsewhere (90). Briefly, cells were disrupted using a beadbeater in the presence of equal volume of acidic phenol:chloroform. After centrifugation, the cell lysate was processed using the RNeasy minikit (Qiagen, Germantown, MD) and an RNase-free DNase I solution (Qiagen) for extraction of total RNA. The RNA samples were shipped on dry ice to SeqCenter (Pittsburgh, PA) for quality check, cDNA preparation, and deep sequencing, yielding up to 12 million paired end reads (2 × 51 bp) per sample. The analysis of the RNA-seq data was performed in software R version 3.5.2 Eggshell Igloo as described previously (90). The compositional matrix of the expression data was normalized with the voom (91) function from the R package limma (92). The statistical analysis of the expression data (Table S10) was conducted using the package edgeR (version 3.24.3). A false-discovery rate (FDR) of 0.05 and a fold-of-change of 2.0 were used as the cutoff values for identification of genes with differential expression, consistent with the published work on H_2O_2

transcriptome in *S. mutans* (36). Findings from this analysis were validated by reverse transcriptase quantitative PCR (RT-qPCR) (30) carried out on 20 selected genes, following a previously published protocol detailed elsewhere (93, 94). The sequencing data from this study have been deposited at NCBI Gene Expression Omnibus (GEO) under the accession numbers GSE279080.

For comparative analysis under different treatments, we obtained the RNA-seq datasets (GEO, GSE98526) of an analysis previously performed on strain UA159 that was treated with 0.5 mM H_2O_2 for 5 min (36). Comparison between transcriptomes was carried out in R statistical language using the package edgeR as done previously (95).

Long-term persistence assay. For comparison of the ability to persist under low-pH and starvation conditions, the cultures of *S. mutans* were each diluted 1000-fold into an FMC medium supplemented with 20 mM glucose, 20 mM fructose, or 19 mM glucose and 1 mM fructose combined. The cultures were incubated at 37°C in an ambient atmosphere supplemented with 5% CO_2 for a duration of 11 days. After one or two days of incubation, a 30-second sonication at 100% power (FB120 water bath sonicator, Fisher Scientific) was applied to all cultures to disperse bacterial chains and aggregates, then a 100-µL aliquot of each culture was removed. The cultures were returned to incubation without any other treatments, and the 100-µL aliquots were each diluted decimally in sterile PBS and plated on BHI agar. After 2 days of incubation, the CFU on each plate were enumerated. Plating was repeated at specified time points thereafter till end of the experiment.

Mixed-species competition in planktonic cultures. For interspecies competition in liquid cultures, differentially marked strains of *S. mutans* (UA159-Km and Δ*fruI::Km*) (96) and *S. sanguinis* (MMZ1945, Em resistant) (97) were each cultured in BHI to the exponential phase (OD_{600} = 0.5). An inoculum of approximately 10^6 CFU/ml of *S. mutans* together with similar numbers of *S. sanguinis* were added to FMC supplemented with 20, or 200 mM glucose or fructose, then cultured for 20 h in a 5%-CO_2 environment at 37°C. At both the start and the end of the incubation, cultures were sonicated for 15 sec, decimally diluted and plated on respective antibiotic plates to enumerate CFU of both species. The competitive index was calculated by following this formula: [SMU(t_{end})/SSA(t_{end})] / [SMU(t_{start})/SSA(t_{start})], with values >1 indicating SMU (*S. mutans*) being more competitive than SSA (*S. sanguinis*), and vice versa.

pH drop and chloramphenicol acetyltransferase (CAT) assay. Glycolytic profiling via pH drop (98) and CAT assay (99) were conducted according to previously published protocols detailed elsewhere.

Statistics. Statistical analysis of data was carried out using the software of Prism (GraphPad of Dotmatics, San Diego, CA)

Acknowledgements

This study was supported by a grant DE12236 from NIDCR and a startup fund from University of Florida to LZ. JL was supported by grants DE032555 and DE019783 from NIDCR. Parts of Fig. 8 were created using BioRender.com.

Figure Legends

Fig. 1 Volcano plots illustrating transcriptomes of four treatments. *S. mutans* UA159 was grown to the exponential phase in a synthetic FMC medium containing 20 mM glucose. The samples were treated for 30 min with 5 mM methylglyoxal, 50 mM fructose, or 50 mM glucose before harvesting for mRNA sequencing. Differential expression analyses were performed against untreated cells using edgeR, with cutoffs for foldchange >2 and FDR <0.05. Upregulated genes are shown in red, and downregulated ones in blue. Results of treatment by H_2O_2 (0.5 mM, 5 min) were from an independent study (36).

Fig. 2 Transcriptomic overlaps among treatments of methylglyoxal, fructose, glucose and H_2O_2. The Venn diagrams show the numbers of shared and unique genes in the genome of UA159, separated into groups of upregulated and downregulated, among treatments of (A) 5 mM methylglyoxal (MG) and 0.5 mM H_2O_2, (B) MG and 50 mM fructose (Fru), (C) MG and 50 mM glucose (Glc50), and (D) all four treatments.

Fig. 3 Fructose impacts metal homeostasis in Δ*zccR* deficient in zinc expulsion. *S. mutans* strains UA159 and its mutant derivatives were diluted from exponential phase cultures into TV supplemented with 20 mM glucose (A) or fructose (B). Mn^{2+} was added at 25 μM ($MnSO_4$). Growth was monitored using a Synergy 2 plate reader maintained at 37°C. Results are average of three biological replicates, each tested in technical duplicates. Error bars denote standard deviations.

Fig. 4 Fructose impacts growth of *spxA1* in a medium-specific manner. *S. mutans* strains UA159 and various mutant derivatives were each diluted from exponential phase cultures into TV (A) or FMC (B, C) supplemented with 20 mM glucose (Glc) or fructose (Fru). Growth was monitored using a Synergy 2 plate reader maintained at 37°C. Results are average of three biological replicates, each tested in technical duplicates. Error bars denote standard deviations.

Fig. 5 Induction of the *sodA* promoter by fructose. (A) Cultures of UA159 harboring a P*sodA::gfp* fusion were diluted into FMC containing specified concentrations (in mM) of glucose (G), fructose (F), or H_2O_2. The cultures were monitored in a Synergy 2 plate reader for green fluorescence and optical densities (OD_{600}) for 20 hours. (B) The same experiment was performed on various mutants derived from UA159/P*sodA::gfp,* using FMC containing 20 mM glucose (G20) or fructose (F20). The relative fluorescence units (RFU) of each culture were recorded as a measure of *sodA* promoter activity, subtracted with RFUs of a control strain (the same genetic background but without the *gfp* fusion) cultured under the same condition, and normalized against corresponding OD_{600} values of the bacterial cultures. Results are the average from three biological replicates, conducted in technical duplicates. Error bars denote standard deviations.

Fig. 6 Fructose promotes long-term survival of *S. mutans*. Cultures of *S. mutans* UA159 (A, B) or Δ*fruI* (B) were diluted into FMC containing 20 mM of glucose (G20) or

764 fructose (F20), or a combination of 19 mM glucose and 1 mM fructose (G19/F1),
765 followed by incubation without medium refreshment for 11 days. At specified time
766 points, an aliquot of culture was removed for CFU enumeration. Each strain was
767 represented by 3 independent cultures, with results presenting average and standard
768 deviation. Statistical significance was assessed using (A) One-Way ANOVA followed
769 with Dunnett's comparisons against G20 samples, and (B) Two-Way ANOVA followed
770 by Tukey's multiple comparisons against G20 samples (*, P<0.05; **, P<0.01; ***,
771 P<0.001; ****, P<0.0001).
772
773 **Fig. 7 Fructose enhances acidogenicity (A) and competitiveness (B) of *S. mutans*.**
774 (A) pH drop assay. UA159 was cultured in TV with 20 mM glucose or fructose to
775 exponential phase, harvested and resuspended in a solution of 50 mM KCl and 1 mM
776 $MgCl_2$, with OD_{600} adjusted to 5.0. The pH was adjusted to 7.2 slowly with 0.1 N KOH to
777 consume intracellular carbohydrate storage. Immediately after addition of 50 mM
778 glucose or fructose, same as the sugar used in the TV medium, the pH of the
779 suspension was monitored continuously on a stirring plate for the next 60 min. Each
780 experiment was repeated three times (Fig. S5), with representative results shown here.
781 After conversion into proton concentrations, area under the curve (AUC, see inset) of
782 each sample was calculated and used to assess statistical significance using Student's
783 *t*-test (*, P < 0.05). (B) Cultures of *S. mutans* wild type UA159 or Δ*fruI* were mixed at 1:1
784 ratio with a differentially marked *S. sanguinis* strain, then diluted at 1:100 into FMC
785 containing glucose (G) or fructose (F), each used at 20 mM or 200 mM. After 24 h of
786 incubation, the cultures were sonicated and used for CFU enumeration. CFUs from both

the start and end of the incubation (Fig. S6) were used to calculate competitive indices. Results were the average of three independent repeats, with error bars denoting standard deviations. Statistical significance was assessed using Two-Way ANOVA followed by Tukey's multiple comparisons (*, $P<0.05$; **, $P<0.01$).

Fig. 8 Fructose metabolism triggers stress response in streptococci. Fructose is internalized by oral streptococci primarily through a F-1-P-generating PTS transporter, FruI, but also through two additional PTS permeases, including EII^{Lev} (LevDEFG) that generates F-6-P. Compared to the glucose pathway, fructose is likely catabolized more rapidly via glycolysis, during which RES such as methylglyoxal is accumulated and impacts cytoplasmic redox balance represented by the ratios of GSH/GSSG and $NADPH/NADP^+$. Increased F-1-P kinase activities (denoted by a plus sign) and reduced expression of F-1,6-bP aldolase (by a minus sign) may further contribute to RES production through impeded F-6-P phosphorylation and increased cleavage of F-6-P into DHA. Also affected are the pools of intracellular metal ions. Sensing these and other not-yet-characterized physiological changes and specific metabolites, the bacterium reprograms a suite of stress responsive genes. The outcomes of exposure to fructose include not only elevated activities in processing RES, through the functions of LguL/GloB and related protein GloA2, but importantly enhanced tolerance to multiple environmental stressors including ROS, RES, acidic pH, toxic metals, and nutrient depletion.

Reference

1. Baker JL, Mark Welch JL, Kauffman KM, McLean JS, He X. 2024. The oral microbiome: diversity, biogeography and human health. Nat Rev Microbiol 22:89-104.
2. Hsu CL, Schnabl B. 2023. The gut-liver axis and gut microbiota in health and liver disease. Nat Rev Microbiol 21:719-733.
3. Willenborg J, Goethe R. 2016. Metabolic traits of pathogenic streptococci. FEBS Lett 590:3905-3919.
4. Bowen WH, Burne RA, Wu H, Koo H. 2018. Oral Biofilms: pathogens, matrix, and polymicrobial interactions in microenvironments. Trends Microbiol 26:229-242.
5. Tanner ACR, Kressirer CA, Rothmiller S, Johansson I, Chalmers NI. 2018. The Caries Microbiome: Implications for Reversing Dysbiosis. Adv Dent Res 29:78-85.
6. Spatafora G, Li Y, He X, Cowan A, Tanner ACR. 2024. The Evolving Microbiome of Dental Caries. Microorganisms 12.
7. Stangvaltaite-Mouhat L, Skudutyte-Rysstad R, Ko H, Stankeviciene I, Aleksejuniene J, Puriene A. 2024. Co-occurrence of dental caries and periodontitis: multilevel modelling approach. BMC Oral Health 24:149.
8. Strauss F-J, Espinoza I, Stähli A, Baeza M, Cortés R, Morales A, Gamonal J. 2019. Dental caries is associated with severe periodontitis in Chilean adults: a cross-sectional study. BMC Oral Health 19:278.

9. Romandini P, Marruganti C, Romandini WG, Sanz M, Grandini S, Romandini M. 2024. Are periodontitis and dental caries associated? A systematic review with meta-analyses. J Clin Periodontol 51:145-157.

10. Tappy L, Lê KA. 2010. Metabolic effects of fructose and the worldwide increase in obesity. Physiol Rev 90:23-46.

11. Azevedo-Martins AK, Santos MP, Abayomi J, Ferreira NJR, Evangelista FS. 2024. The Impact of Excessive Fructose Intake on Adipose Tissue and the Development of Childhood Obesity. Nutrients 16.

12. Gillespie KM, White MJ, Kemps E, Moore H, Dymond A, Bartlett SE. 2023. The Impact of Free and Added Sugars on Cognitive Function: A Systematic Review and Meta-Analysis. Nutrients 16.

13. Siddiqui SH, Rossi NF. 2024. Acute Intake of Fructose Increases Arterial Pressure in Humans: A Meta-Analysis and Systematic Review. Nutrients 16.

14. Staltner R, Burger K, Baumann A, Bergheim I. 2023. Fructose: a modulator of intestinal barrier function and hepatic health? Eur J Nutr 62:3113-3124.

15. Ting KKY. 2024. Fructose-induced metabolic reprogramming of cancer cells. Front Immunol 15:1375461.

16. Johnson RJ, Lanaspa MA, Sanchez-Lozada LG, Tolan D, Nakagawa T, Ishimoto T, Andres-Hernando A, Rodriguez-Iturbe B, Stenvinkel P. 2023. The fructose survival hypothesis for obesity. Philos Trans R Soc Lond B Biol Sci 378:20220230.

17. Wen ZT, Browngardt C, Burne RA. 2001. Characterization of two operons that encode components of fructose-specific enzyme II of the

852 sugar:phosphotransferase system of *Streptococcus mutans*. FEMS Microbiol Lett
853 205:337-42.
854 18. Loo CY, Mitrakul K, Voss IB, Hughes CV, Ganeshkumar N. 2003. Involvement of
855 an inducible fructose phosphotransferase operon in *Streptococcus gordonii*
856 biofilm formation. J Bacteriol 185:6241-54.
857 19. Cao Q, Dong Y, Guo C, Ji S, Nie M, Liu G, Wan X, Lu C, Liu Y. 2023. *luxS*
858 contributes to intramacrophage survival of *Streptococcus agalactiae* by positively
859 affecting the expression of *fruRKI* operon. Vet Res 54:83.
860 20. Zeng L, Chakraborty B, Farivar T, Burne RA. 2017. Coordinated regulation of the
861 EII^{Man} and *fruRKI* operons of *Streptococcus mutans* by global and fructose-
862 specific pathways. Appl Environ Microbiol 83:e01403-17.
863 21. Jesionowski AM, Mansfield JM, Brittan JL, Jenkinson HF, Vickerman MM. 2016.
864 Transcriptome analysis of *Streptococcus gordonii* Challis DL1 indicates a role for
865 the biofilm-associated *fruRBA* operon in response to *Candida albicans*. Mol Oral
866 Microbiol 31:314-328.
867 22. Valdes KM, Sundar GS, Vega LA, Belew AT, Islam E, Binet R, El-Sayed NM, Le
868 Breton Y, McIver KS. 2016. The *fruRBA* operon is necessary for group A
869 streptococcal growth in fructose and for resistance to neutrophil killing during
870 growth in whole human blood. Infect Immun 84:1016-31.
871 23. Zeng L, Burne RA. 2019. Essential roles of the *sppRA* fructose-phosphate
872 phosphohydrolase operon in carbohydrate metabolism and virulence expression
873 by *Streptococcus mutans*. J Bacteriol 201:e00586-18.

24. Tanzer JM, Thompson A, Wen ZT, Burne RA. 2006. *Streptococcus mutans*: fructose transport, xylitol resistance, and virulence. J Dent Res 85:369-73.

25. Gauthier L, Mayrand D, Vadeboncoeur C. 1984. Isolation of a novel protein involved in the transport of fructose by an inducible phosphoenolpyruvate fructose phosphotransferase system in *Streptococcus mutans*. J Bacteriol 160:755-63.

26. Zeng L, Wen ZT, Burne RA. 2006. A novel signal transduction system and feedback loop regulate fructan hydrolase gene expression in *Streptococcus mutans*. Mol Microbiol 62:187-200.

27. Ajdic D, McShan WM, McLaughlin RE, Savic G, Chang J, Carson MB, Primeaux C, Tian R, Kenton S, Jia H, Lin S, Qian Y, Li S, Zhu H, Najar F, Lai H, White J, Roe BA, Ferretti JJ. 2002. Genome sequence of *Streptococcus mutans* UA159, a cariogenic dental pathogen. Proc Natl Acad Sci U S A 99:14434-9.

28. Xu P, Alves JM, Kitten T, Brown A, Chen Z, Ozaki LS, Manque P, Ge X, Serrano MG, Puiu D, Hendricks S, Wang Y, Chaplin MD, Akan D, Paik S, Peterson DL, Macrina FL, Buck GA. 2007. Genome of the opportunistic pathogen *Streptococcus sanguinis*. J Bacteriol 189:3166-3175.

29. Makarewicz O, Lucas M, Brandt C, Herrmann L, Albersmeier A, Rückert C, Blom J, Goesmann A, van der Linden M, Kalinowski J, Pletz MW. 2017. Whole Genome Sequencing of 39 Invasive *Streptococcus pneumoniae* Sequence Type 199 Isolates Revealed Switches from Serotype 19A to 15B. PLoS ONE 12:e0169370.

30. Zeng L, Noeparvar P, Burne RA, Glezer BS. 2024. Genetic characterization of glyoxalase pathway in oral streptococci and its contribution to interbacterial competition. J Oral Microbiol 16:2322241.

31. Zhang MM, Ong CL, Walker MJ, McEwan AG. 2016. Defence against methylglyoxal in Group A *Streptococcus*: a role for Glyoxylase I in bacterial virulence and survival in neutrophils? Pathog Dis 74.

32. Cooper RA. 1984. Metabolism of methylglyoxal in microorganisms. Annu Rev Microbiol 38:49-68.

33. Zeng L, Burne RA. 2016. Sucrose- and fructose-specific effects on the transcriptome of *Streptococcus mutans*, as determined by RNA sequencing. Appl Environ Microbiol 82:146-56.

34. Zeng L, Burne RA. 2013. Comprehensive mutational analysis of sucrose-metabolizing pathways in *Streptococcus mutans* reveals novel roles for the sucrose phosphotransferase system permease. J Bacteriol 195:833-43.

35. Kajfasz JK, Zuber P, Ganguly T, Abranches J, Lemos JA. 2021. Increased oxidative stress tolerance of a spontaneously occurring *perR* gene mutation in *Streptococcus mutans* UA159. J Bacteriol 203.

36. Kajfasz JK, Ganguly T, Hardin EL, Abranches J, Lemos JA. 2017. Transcriptome responses of *Streptococcus mutans* to peroxide stress: identification of novel antioxidant pathways regulated by Spx. Sci Rep 7:16018.

37. Noctor G, Foyer CH. 1998. ASCORBATE AND GLUTATHIONE: Keeping Active Oxygen Under Control. Annu Rev Plant Physiol Plant Mol Biol 49:249-279.

918 38. Zheng X, Zhang K, Zhou X, Liu C, Li M, Li Y, Wang R, Li Y, Li J, Shi W, Xu X.
919 2013. Involvement of *gshAB* in the interspecies competition within oral biofilm. J
920 Dent Res 92:819-24.
921 39. Ellepola K, Huang X, Riley RP, Bitoun JP, Wen ZT. 2021. *Streptococcus mutans*
922 lacking *sufCDSUB* Is viable, but displays major defects in growth, stress
923 tolerance responses and biofilm formation. Front Microbiol 12:671533.
924 40. Wu X, Hou J, Chen X, Chen X, Zhao W. 2016. Identification and functional
925 analysis of the L-ascorbate-specific enzyme II complex of the
926 phosphotransferase system in *Streptococcus mutans*. BMC Microbiol 16:51.
927 41. Makhlynets O, Boal AK, Rhodes DV, Kitten T, Rosenzweig AC, Stubbe J. 2014.
928 *Streptococcus sanguinis* class Ib ribonucleotide reductase: high activity with both
929 iron and manganese cofactors and structural insights. J Biol Chem 289:6259-72.
930 42. Rhodes DV, Crump KE, Makhlynets O, Snyder M, Ge X, Xu P, Stubbe J, Kitten T.
931 2014. Genetic characterization and role in virulence of the ribonucleotide
932 reductases of *Streptococcus sanguinis*. J Biol Chem 289:6273-87.
933 43. Stewart LJ, Ong CY, Zhang MM, Brouwer S, McIntyre L, Davies MR, Walker MJ,
934 McEwan AG, Waldron KJ, Djoko KY. 2020. Role of Glutathione in Buffering
935 Excess Intracellular Copper in *Streptococcus pyogenes*. mBio 11.
936 44. Griswold AR, Chen YY, Burne RA. 2004. Analysis of an agmatine deiminase
937 gene cluster in *Streptococcus mutans* UA159. J Bacteriol 186:1902-4.
938 45. Seaton K, Ahn S-J, Burne RA. 2014. Regulation of competence and gene
939 expression in *Streptococcus mutans* by the RcrR transcriptional regulator. Mol
940 Oral Microbiol 30:147-59.

941 46. Merritt J, Qi F, Shi W. 2005. A unique nine-gene *comY* operon in *Streptococcus*
942 *mutans*. Microbiology 151:157-66.
943 47. Merritt J, Qi F. 2012. The mutacins of *Streptococcus mutans*: regulation and
944 ecology. Mol Oral Microbiol 27:57-69.
945 48. Banu LD, Conrads G, Rehrauer H, Hussain H, Allan E, van der Ploeg JR. 2010.
946 The *Streptococcus mutans* serine/threonine kinase, PknB, regulates competence
947 development, bacteriocin production, and cell wall metabolism. Infect Immun
948 78:2209-20.
949 49. Leung V, Ajdic D, Koyanagi S, Levesque CM. 2015. The formation of
950 *Streptococcus mutans* persisters induced by the quorum-sensing peptide
951 pheromone is affected by the LexA regulator. J Bacteriol 197:1083-94.
952 50. Alves LA, Ganguly T, Harth-Chu EN, Kajfasz J, Lemos JA, Abranches J, Mattos-
953 Graner RO. 2020. PepO is a target of the two-component systems VicRK and
954 CovR required for systemic virulence of *Streptococcus mutans*. Virulence 11:521-
955 536.
956 51. Underhill SAM, Shields RC, Burne RA, Hagen SJ. 2019. Carbohydrate and PepO
957 control bimodality in competence development by *Streptococcus mutans*. Mol
958 Microbiol 112:1388-1402.
959 52. Serbanescu MA, Cordova M, Krastel K, Flick R, Beloglazova N, Latos A, Yakunin
960 AF, Senadheera DB, Cvitkovitch DG. 2015. Role of the *Streptococcus mutans*
961 CRISPR-cas systems in immunity and cell physiology. J Bacteriol 197:749-761.

962 53. Lemme A, Sztajer H, Wagner-Döbler I. 2010. Characterization of *mleR*, a positive
963 regulator of malolactic fermentation and part of the acid tolerance response in
964 *Streptococcus mutans*. BMC Microbiol 10:58.
965 54. Sheng J, Marquis RE. 2007. Malolactic fermentation by *Streptococcus mutans*.
966 FEMS Microbiol Lett 272:196-201.
967 55. King S, Quick A, King K, Walker AR, Shields RC. 2022. Activation of TnSmu1, an
968 integrative and conjugative element, by an ImmR-like transcriptional regulator in
969 *Streptococcus mutans*. Microbiology (Reading) 168.
970 56. Ganguly T, Peterson AM, Burkholder M, Kajfasz JK, Abranches J, Lemos JA.
971 2022. ZccE is a novel P-type ATPase that protects *Streptococcus mutans* against
972 zinc intoxication. PLoS Pathog 18:e1010477.
973 57. Zeng L, Das S, Burne RA. 2010. Utilization of lactose and galactose by
974 *Streptococcus mutans*: transport, toxicity, and carbon catabolite repression. J
975 Bacteriol 192:2434-44.
976 58. Sato Y, Yamamoto Y, Kizaki H. 2000. Construction of region-specific partial
977 duplication mutants (merodiploid mutants) to identify the regulatory gene for the
978 glucan-binding protein C gene *in vivo in Streptococcus mutans*. FEMS Microbiol
979 Lett 186:187-91.
980 59. Tao L, Sutcliffe IC, Russell RR, Ferretti JJ. 1993. Transport of sugars, including
981 sucrose, by the *msm* transport system of *Streptococcus mutans*. J Dent Res
982 72:1386-90.

983 60. Costa Oliveira BE, Ricomini Filho AP, Burne RA, Zeng L. 2021. The Route of
984 Sucrose Utilization by *Streptococcus mutans* Affects Intracellular Polysaccharide
985 Metabolism. Front Microbiol 12:636684.
986 61. Sato Y, Okamoto-Shibayama K, Azuma T. 2013. The *malQ* gene is essential for
987 starch metabolism in *Streptococcus mutans*. J Oral Microbiol 5:21285.
988 62. Kremer BH, van der Kraan M, Crowley PJ, Hamilton IR, Brady LJ, Bleiweis AS.
989 2001. Characterization of the *sat* operon in *Streptococcus mutans*: evidence for a
990 role of Ffh in acid tolerance. J Bacteriol 183:2543-52.
991 63. Gong Y, Tian XL, Sutherland T, Sisson G, Mai J, Ling J, Li YH. 2009. Global
992 transcriptional analysis of acid-inducible genes in *Streptococcus mutans*: multiple
993 two-component systems involved in acid adaptation. Microbiology 155:3322-32.
994 64. Baker JL, Faustoferri RC, Quivey RG, Jr. 2017. Acid-adaptive mechanisms of
995 *Streptococcus mutans*-the more we know, the more we don't. Mol Oral Microbiol
996 32:107-117.
997 65. Baker JL, Abranches J, Faustoferri RC, Hubbard CJ, Lemos JA, Courtney MA,
998 Quivey R, Jr. 2015. Transcriptional profile of glucose-shocked and acid-adapted
999 strains of *Streptococcus mutans*. Mol Oral Microbiol doi:10.1111/omi.12110.
1000 66. Burne RA, Wen ZT, Chen YY, Penders JE. 1999. Regulation of expression of the
1001 fructan hydrolase gene of *Streptococcus mutans* GS-5 by induction and carbon
1002 catabolite repression. J Bacteriol 181:2863-71.
1003 67. Kajfasz JK, Rivera-Ramos I, Scott-Anne K, Gregoire S, Abranches J, Lemos JA.
1004 2015. Transcription of Oxidative Stress Genes Is Directly Activated by SpxA1

1005 and, to a Lesser Extent, by SpxA2 in *Streptococcus mutans*. J Bacteriol
1006 197:2160-2170.
1007 68. Kreth J, Merritt J, Shi W, Qi F. 2005. Competition and coexistence between
1008 *Streptococcus mutans* and *Streptococcus sanguinis* in the dental biofilm. J
1009 Bacteriol 187:7193-7203.
1010 69. Culp DJ, Hull W, Bremgartner MJ, Atherly TA, Christian KN, Killeen M, Dupuis
1011 MR, Schultz AC, Chakraborty B, Lee K, Wang DS, Afzal V, Chen T, Burne RA.
1012 2020. *In vivo* colonization with candidate oral probiotics attenuates colonization
1013 and virulence of *Streptococcus mutans*. Appl Environ Microbiol 87.
1014 70. Velsko IM, Chakraborty B, Nascimento MM, Burne RA, Richards VP. 2018.
1015 Species designations belie phenotypic and genotypic heterogeneity in oral
1016 streptococci. mSystems 3:e00158-18.
1017 71. Miller JH, Avilés-Reyes A, Scott-Anne K, Gregoire S, Watson GE, Sampson E,
1018 Progulske-Fox A, Koo H, Bowen WH, Lemos JA, Abranches J. 2015. The
1019 collagen binding protein Cnm contributes to oral colonization and cariogenicity of
1020 *Streptococcus mutans* OMZ175. Infect Immun 83:2001-10.
1021 72. Papadimitriou K, Alegria A, Bron PA, de Angelis M, Gobbetti M, Kleerebezem M,
1022 Lemos JA, Linares DM, Ross P, Stanton C, Turroni F, van Sinderen D, Varmanen
1023 P, Ventura M, Zuniga M, Tsakalidou E, Kok J. 2016. Stress physiology of lactic
1024 acid bacteria. Microbiol Mol Biol Rev 80:837-90.
1025 73. Abranches J, Zeng L, Kajfasz JK, Palmer SR, Chakraborty B, Wen ZT, Richards
1026 VP, Brady LJ, Lemos JA. 2018. Biology of oral streptococci. *In* Fischetti VA,

1027 Novick RP, Ferretti J, Portnoy DA, Braunstein M, Rood JI (ed), Gram-positive
1028 pathogens doi:doi:10.1128/microbiolspec.GPP3-0042-2018. Microbiol Spectrum.
1029 74. Liu C, Niu Y, Zhou X, Zhang K, Cheng L, Li M, Li Y, Wang R, Yang Y, Xu X. 2013.
1030 Hyperosmotic response of *Streptococcus mutans*: from microscopic physiology
1031 to transcriptomic profile. BMC Microbiology 13:275.
1032 75. Abranches J, Lemos JA, Burne RA. 2006. Osmotic stress responses of
1033 *Streptococcus mutans* UA159. FEMS Microbiol Lett 255:240-6.
1034 76. Kunii M, Arimoto T, Hasegawa T, Kuwata H, Igarashi T. 2014. Role of protease
1035 maturation lipoprotein in osmoadaptation of *Streptococcus mutans*. FEMS
1036 Microbiol Lett 356:45-52.
1037 77. Lee C, Park C. 2017. Bacterial responses to glyoxal and methylglyoxal: reactive
1038 electrophilic species. Int J Mol Sci 18.
1039 78. Akbari MS, Joyce LR, Spencer BL, Brady A, McIver KS, Doran KS. 2025.
1040 Identification of glyoxalase A in group B *Streptococcus* and its contribution to
1041 methylglyoxal tolerance and virulence. Infect Immun doi:10.1128/iai.00540-
1042 24:e0054024.
1043 79. Darwin KH, Stanley SA. 2022. The aldehyde hypothesis: metabolic intermediates
1044 as antimicrobial effectors. Open Biology 12:220010.
1045 80. Doi Y. 2019. Glycerol metabolism and its regulation in lactic acid bacteria. Appl
1046 Microbiol Biotechnol 103:5079-5093.
1047 81. Taylor ZA, Chen P, Noeparvar P, Pham DN, Walker AR, Kitten T, Zeng L. 2024.
1048 Glycerol metabolism contributes to competition by oral streptococci through
1049 production of hydrogen peroxide. J Bacteriol 206:e0022724.

1050 82. Monniot C, Zébré AC, Aké FMD, Deutscher J, Milohanic E. 2012. Novel Listerial
1051 Glycerol Dehydrogenase- and Phosphoenolpyruvate-Dependent
1052 Dihydroxyacetone Kinase System Connected to the Pentose Phosphate
1053 Pathway. J Bacteriol 194:4972-4982.
1054 83. Li HK, Zhi X, Vieira A, Whitwell HJ, Schricker A, Jauneikaite E, Li H, Yosef A,
1055 Andrew I, Game L, Turner CE, Lamagni T, Coelho J, Sriskandan S. 2023.
1056 Characterization of emergent toxigenic M1(UK) *Streptococcus pyogenes* and
1057 associated sublineages. Microb Genom 9.
1058 84. Xiao T, Xia W. 2013. Cariogenicity of high fructose corn syrup: an experimental
1059 study on rats. Chin J Cons Dent 23:446–449.
1060 85. Sun M, Kang Q, Li T, Huang L, Jiang Y, Xia W-W. 2014. Effect of high-fructose
1061 corn syrup on *Streptococcus mutans* virulence gene expression and on tooth
1062 demineralization. Eur J Oral Sci 122:216-22.
1063 86. Kawasaki T, Akanuma H, Yamanouchi T. 2002. Increased fructose concentrations
1064 in blood and urine in patients with diabetes. Diabetes Care 25:353-7.
1065 87. Tanzer JM, Chassy BM, Krichevsky MI. 1971. Sucrose metabolism by
1066 *Streptococcus mutans*, SL-I. Biochim Biophys Acta 261:379-87.
1067 88. Terleckyj B, Willett NP, Shockman GD. 1975. Growth of several cariogenic strains
1068 of oral streptococci in a chemically defined medium. Infect Immun 11:649-55.
1069 89. Zeng L, Chen L, Burne RA. 2018. Preferred hexoses influence long-term memory
1070 in and induction of lactose catabolism by *Streptococcus mutans*. Appl Environ
1071 Microbiol 84:e00864-18.

90. Chen L, Walker AR, Burne RA, Zeng L. 2020. Amino sugars reshape interactions between *Streptococcus mutans* and *Streptococcus gordonii*. Appl Environ Microbiol 87:e01459-20.

91. Law CW, Chen Y, Shi W, Smyth GK. 2014. voom: Precision weights unlock linear model analysis tools for RNA-seq read counts. Genome Biol 15:R29.

92. Ritchie ME, Phipson B, Wu D, Hu Y, Law CW, Shi W, Smyth GK. 2015. limma powers differential expression analyses for RNA-sequencing and microarray studies. Nucleic Acids Res 43:e47.

93. Zeng L, Walker AR, Lee K, Taylor ZA, Burne RA. 2021. Spontaneous mutants of *Streptococcus sanguinis* with defects in the glucose-PTS show enhanced post-exponential phase fitness. J Bacteriol 203:JB0037521.

94. Schmittgen TD, Livak KJ. 2008. Analyzing real-time PCR data by the comparative C_T method. Nat Protocols 3:1101-8.

95. Ranjit DK, Moye ZD, Rocha FG, Ottenberg G, Nichols FC, Kim HM, Walker AR, Gibson FC, 3rd, Davey ME. 2022. Characterization of a Bacterial Kinase That Phosphorylates Dihydrosphingosine to Form dhS1P. Microbiol Spectr 10:e0000222.

96. Chen L, Chakraborty B, Zou J, Burne RA, Zeng L. 2019. Amino sugars modify antagonistic interactions between commensal oral streptococci and *Streptococcus mutans*. Appl Environ Microbiol 85:e00370-19.

97. Zeng L, Walker AR, Burne RA, Taylor ZA. 2022. Glucose phosphotransferase system modulates pyruvate metabolism, bacterial fitness, and microbial ecology in oral streptococci. J Bacteriol 205:e0035222.

98. Moye ZD, Zeng L, Burne RA. 2014. Modification of gene expression and virulence traits in *Streptococcus mutans* in response to carbohydrate availability. Appl Environ Microbiol 80:972-985.

99. Zeng L, Burne RA. 2008. Multiple sugar: phosphotransferase system permeases participate in catabolite modification of gene expression in *Streptococcus mutans*. Mol Microbiol 70:197-208.

100. Huang X, Palmer SR, Ahn SJ, Richards VP, Williams ML, Nascimento MM, Burne RA. 2016. A highly arginolytic *Streptococcus* species that potently antagonizes *Streptococcus mutans*. Appl Environ Microbiol 82:2187-201.

Table 1. Relative expression of selected genes in *S. mutans* UA159 WT and Δ*fruI* (shaded) with specified treatments. After growing to mid-exponential phase (OD_{600} = 0.5) in FMC-Glc (20 mM glucose) at 37˚C in 5% CO_2, bacterial cultures were each treated with: Fru50, 50 mM fructose for 5 or 30 min; MG, 5 mM methylglyoxal for 30 min; H_2O_2, 0.5 mM hydrogen peroxide for 5 or 30 min; or Glc50, 50 mM glucose for 30 min. All values were relative to the untreated WT cultivated with FMC-Glc (second column). Exponential phase cultures of UA159 in FMC-Fru (20 mM fructose) were included as additional controls. Results are average from 3 biological replicates. Asterisks denote statistical significance assessed by One-Way ANOVA ((*, *P* <0.05; **, *P* <0.01; ***, *P* <0.001; ****, *P* <0.0001). NT, not tested.

Genes	FMC-Glc cultures	FMC-Fru cultures	FMC-Glc cultures treated with the following						
			Fru50 5 min	Fru50 30 min	Δ*fruI* Fru50 30 min	MG 30 min	H_2O_2 5 min	H_2O_2 30 min	Glc50 30 min
lguL	1.00	2.27**	2.32**	2.87***	6.66****	2.06*	0.84	5.68****	2.31**
phoR	1.01	1.80	NT	1.64	2.74**	2.68**	0.97	NT	1.47
nlmA	1.01	3.86***	0.41	0.52	0.62	0.24	0.14*	0.43	NT
sloA	1.02	0.29****	0.29****	0.10****	0.04****	0.35****	0.06****	0.20****	0.56***
sloC	1.01	1.66*	NT	NT	NT	0.79	0.45	NT	NT
celB	1.16	0.38*	0.10**	0.06**	4.36****	0.05**	0.22**	0.17**	0.44*
mreC	1.00	0.85	0.61****	0.47****	0.44****	0.07****	0.45****	0.48****	0.52****
lexA	1.02	3.25*	2.04	9.17****	9.03****	6.32****	2.77	11.70****	NT
scnK	1.00	4.78**	5.16***	3.26*	5.56***	6.06***	5.64***	8.41****	1.67
gbpC	1.00	7.62****	6.22****	3.00*	2.32	4.01***	2.12	11.36****	NT
tpx	1.00	3.28	14.64****	NT	NT	10.01****	6.26**	23.32****	NT
ahpF	1.01	5.54*	6.35**	5.62**	11.13****	11.54****	6.17**	11.32****	0.92
copY	1.00	1.06	0.84	1.72	2.27	10.78****	1.21	1.18	1.75
nrdG	1.00	1.76	1.67	0.59	0.41	9.43****	0.48	0.80	NT
gshAB	1.00	1.15	1.33**	2.62****	2.27****	1.24	0.95	1.66****	2.02****
sppA	1.00	NT	3.87***	36.92****	0.71	NT	NT	1.21	NT
SMU.127	1.00	5.37*	4.63*	NT	NT	4.87*	2.91	8.93****	NT
SMU.383c	1.00	0.98	1.96***	NT	NT	2.19****	0.34**	2.08***	NT
SMU.667	1.00	1.75	7.36****	2.97****	0.97	5.68****	2.54***	5.54****	1.76
SMU.679	1.06	2.01*	3.76****	2.64***	1.29	4.55****	1.19	3.32****	1.83

Table 2. pH and final OD_{600} of 20-h TV cultures.

Strains	Sugars	Resting pH			Final OD_{600}		
		20 mM	100 mM	200 mM	20 mM	100 mM	200 mM
SMU_UA159	Glucose	4.92	4.93	4.93	0.83	0.72	0.57
	Fructose	4.76****	4.82**	4.81***	0.82	0.73	0.64****
SSA_SK36	Glucose	6.5	6.15	5.70	0.34	0.41	0.45
	Fructose	6.55	ND	ND	0.27***	0.03****	0.00****
SSA_BCC23	Glucose	6.09	6.01	5.93	0.43	0.37	0.31
	Fructose	5.76***	ND	ND	0.49*	0.20****	0.02****
SDE_BCC10	Glucose	5.48	5.08	5.49	0.63	0.69	0.43
	Fructose	ND	ND	ND	0.28****	0.14****	0.00****
SOR_BCC11	Glucose	5.72	5.65	5.72	0.56	0.52	0.4
	Fructose	5.09****	5.56	ND	0.66****	0.55	0.01****
SPA_BCC15	Glucose	6.53	6.45	6.38	0.12	0.11	0.09
	Fructose	ND	ND	ND	0.02***	0.00***	0.00**
SMI_BCC2	Glucose	4.75	4.73	4.77	0.74	0.65	0.56
	Fructose	4.87**	4.87***	4.87**	0.61****	0.54****	0.47****
SGO_BCC9	Glucose	4.95	4.90	4.91	0.81	0.66	0.54
	Fructose	4.87	5.03	5.97****	0.70****	0.68	0.46***
A12_BCC21	Glucose	5.62	5.37	5.48	0.65	0.56	0.46
	Fructose	5.16***	5.36	ND	0.64	0.54	0.28****
SCR_BCC41	Glucose	6.20	5.93	5.85	0.5	0.47	0.42
	Fructose	5.69****	5.95	ND	0.51	0.41	0.10****
SIN_BCA19	Glucose	5.28	5.12	5.18	0.66	0.58	0.48
	Fructose	5.11***	5.01*	5.14	0.61****	0.55**	0.48

Results show the averages of four independent cultures. Statistical significance was determined using Two-Way ANOVA followed by Bonferroni's test for comparisons with glucose cultures of the same concentration (*, P <0.05; **, P <0.01; ***, P <0.001; ****, P <0.0001). ND, not determined due to lack of substantial growth (in red). SMU, *S. mutans*; SSA, *S. sanguinis*; SDE, *S. dentisani*; SOR, *S. oralis*; SPA, *S. parasanguinis*; SMI, *S. mitis*; SGO, *S. gordonii;* A12*, S. sp. A12;* SCR*, S. cristatus;* SIN*, S. intermedius* (70, 100).

Table 3. Bacterial strains used in this study (excluding clinical isolates used in Table 2).

Strains	Relevant characteristics[a]	Source or reference
S. mutans UA159	*S. mutans* wild type, *perR*$^+$	ATCC 700610
MMZ1654	UA159 *fruI::Km*	From UA159
MMZ2120	UA159 *fruI::Em*	From UA159
Δ*zccR*	UA159 *zccR::Sp*	(56)
MMZ2156	UA159 *zccR::Sp fruI::Km*	From Δ*zccR*
Δ*spxA1*	UA159 *spxA1::Sp*	(36)
MMZ2161	UA159 *spxA1::Sp fruI::Em*	From Δ*spxA1*
MMZ2162	UA159 *spxA1::Sp levD::Em*	From Δ*spxA1*
Δ*spxA2*	UA159 *spxA2::Em*	(36)
MMZ2158	UA159 *sodA::gfp* fusion (*Km*)	From UA159
MMZ2160	UA159 *spxA1::Sp sodA::gfp* fusion	From Δ*spxA1*
MMZ2159	UA159 *fruI::Em sodA::gfp* fusion	From MMZ2120
MMZ2173	UA159 *levD::Em sodA::gfp* fusion	From MMZ2158
MMZ799	UA159 *fruR::cat* fusion (*Km*)	(20)
UA159-Km	UA159 *gtfA::Km*	(96)
S. sanguinis SK36	*S. sanguinis* wild type	Kitten laboratory
MMZ1945	SK36 *gtfP::Em*	(97)

[a] *Km, Em,* and *Sp*: resistance against kanamycin, erythromycin, and spectinomycin, respectively.

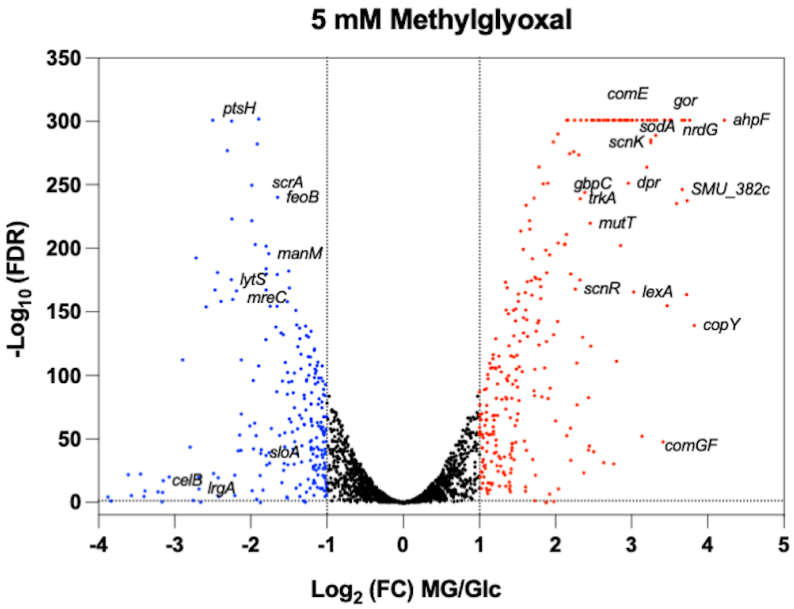
5 mM Methylglyoxal
-Log10 (FDR)
Log2 (FC) MG/Glc
ptsH
scrA
feoB
manM
lytS
mreC
sloA
celB
lrgA
comE
gor
sodA
nrdG
ahpF
scnK
gbpC
trkA
dpr
SMU_382c
mutT
scnR
lexA
copY
comGF

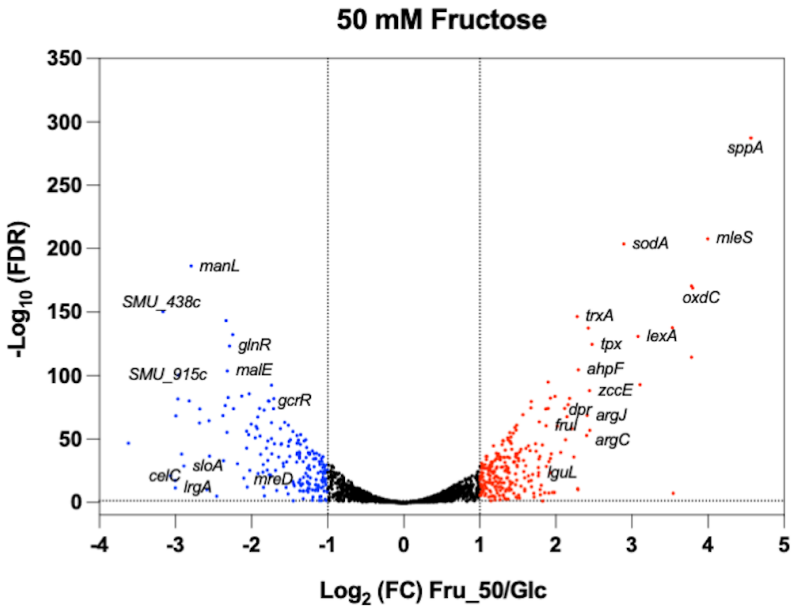
50 mM Fructose
-Log10 (FDR)
Log2 (FC) Fru_50/Glc
sppA
sodA
mleS
manL
oxdC
SMU_438c
trxA
lexA
tpx
glnR
ahpF
SMU_915c
malE
zccE
gcrR
dpr
argJ
frul
argC
celC
sloA
lrgA
mreD
lguL

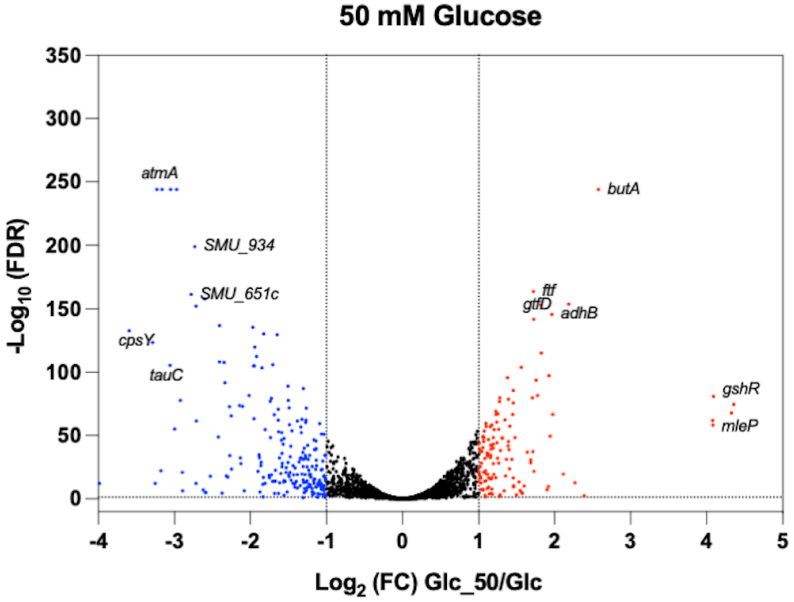
50 mM Glucose
-Log10 (FDR)
Log2 (FC) Glc_50/Glc
atmA
butA
SMU_934
SMU_651c
ftf
gtfD
adhB
cpsY
tauC
gshR
mleP

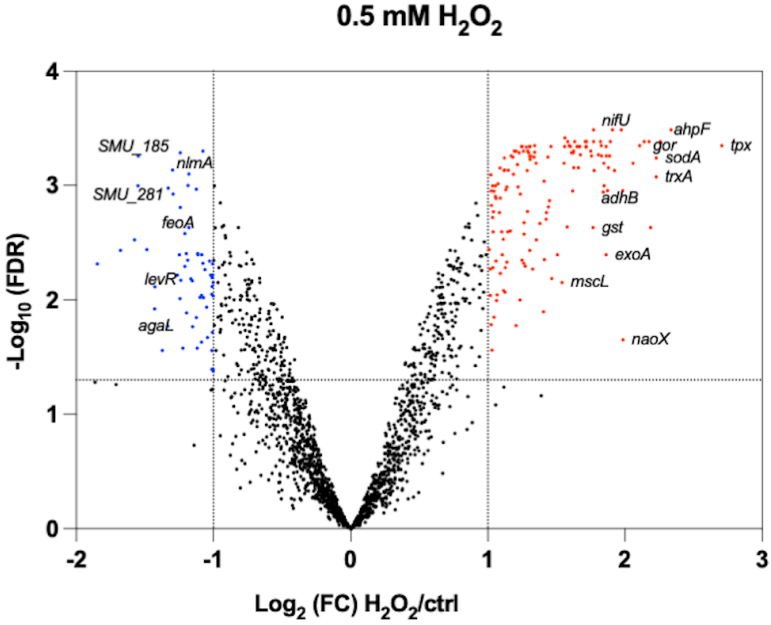
0.5 mM H2O2
-Log10 (FDR)
Log2 (FC) H2O2/ctrl
nifU
ahpF
gor
sodA
trxA
tpx
SMU_185
nlmA
SMU_281
adhB
feoA
gst
exoA
levR
mscL
agaL
naoX

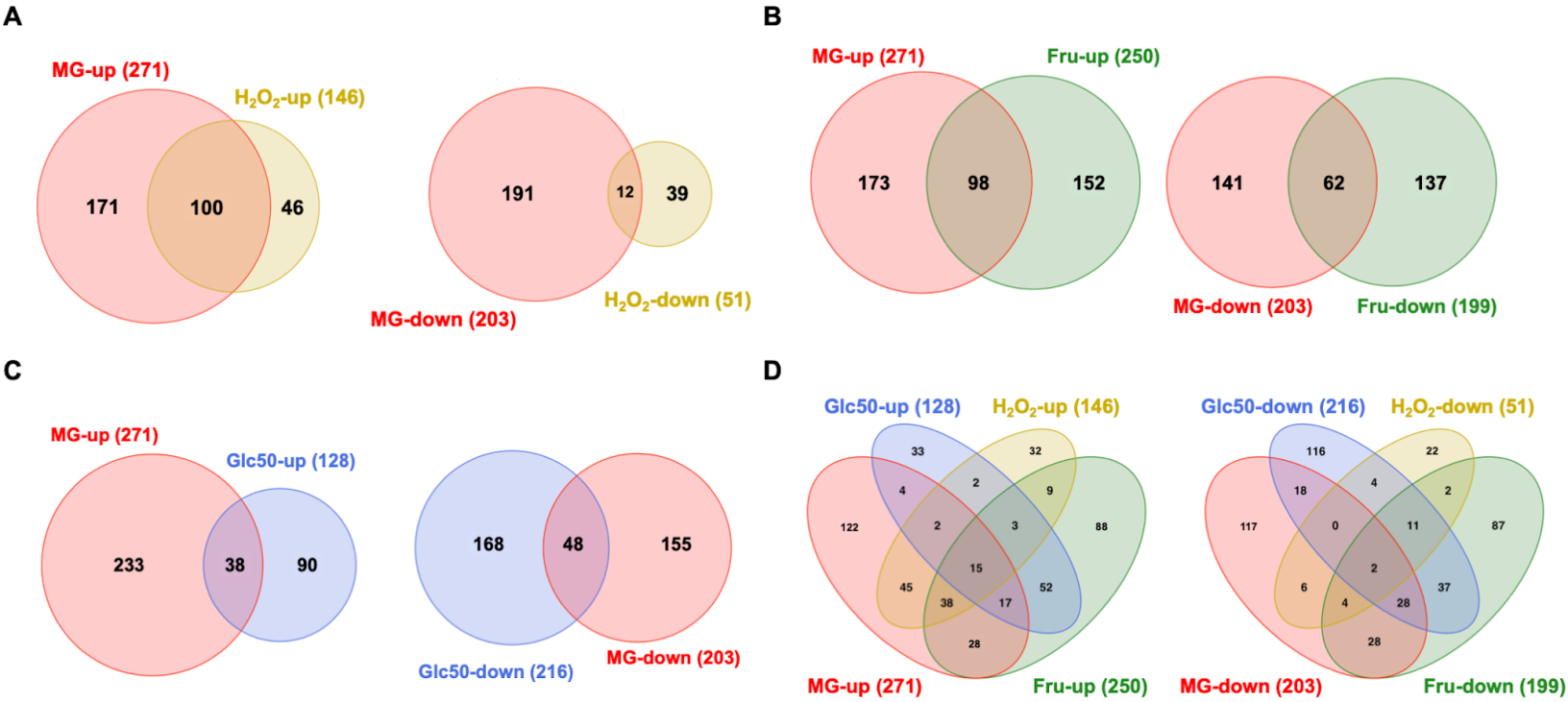
A
MG-up (271)
H_2O_2-up (146)
171
100
46
191
12
39
MG-down (203)
H_2O_2-down (51)
B
MG-up (271)
Fru-up (250)
173
98
152
141
62
137
MG-down (203)
Fru-down (199)
C
MG-up (271)
Glc50-up (128)
233
38
90
168
48
155
Glc50-down (216)
MG-down (203)
D
Glc50-up (128)
H_2O_2-up (146)
33
32
4
2
9
122
2
3
88
15
45
38
17
52
28
MG-up (271)
Fru-up (250)
Glc50-down (216)
H_2O_2-down (51)
116
22
18
4
2
117
0
11
87
2
6
4
28
37
28
MG-down (203)
Fru-down (199)

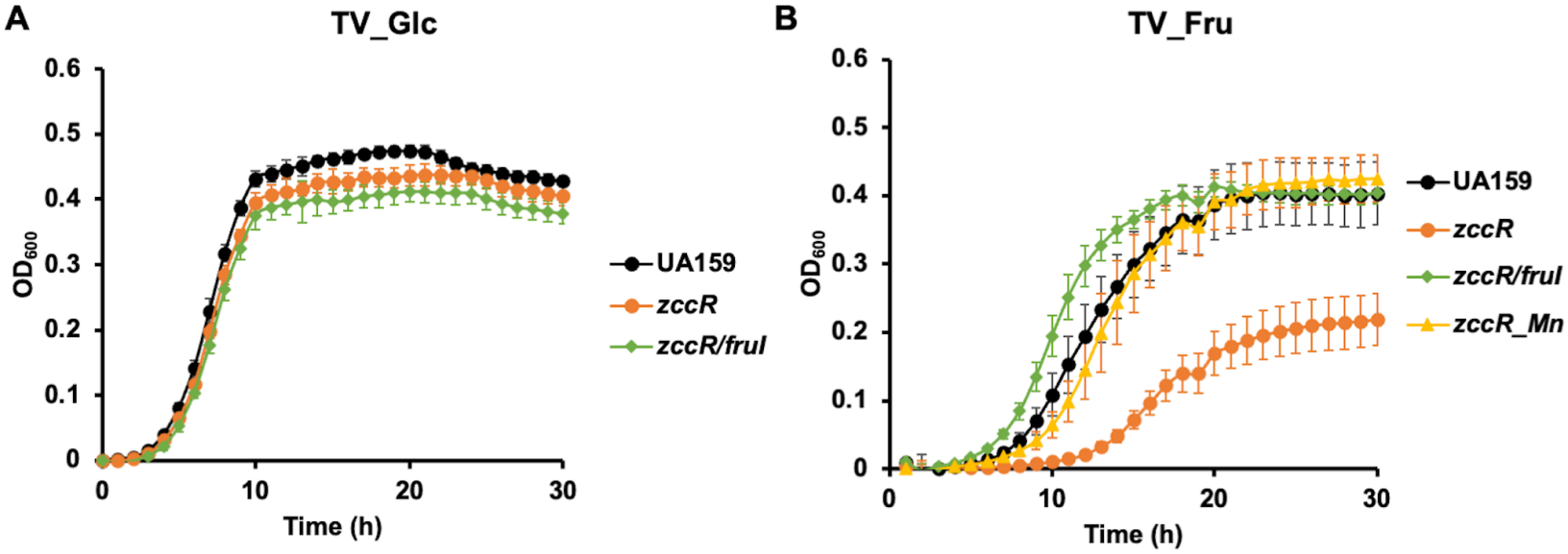
A
TV_Glc
0.6
0.5
0.4
0.3
0.2
0.1
0
OD600
0
10
20
30
Time (h)
UA159
zccR
zccR/frul
B
TV_Fru
0.6
0.5
0.4
0.3
0.2
0.1
0
OD600
0
10
20
30
Time (h)
UA159
zccR
zccR/frul
zccR_Mn

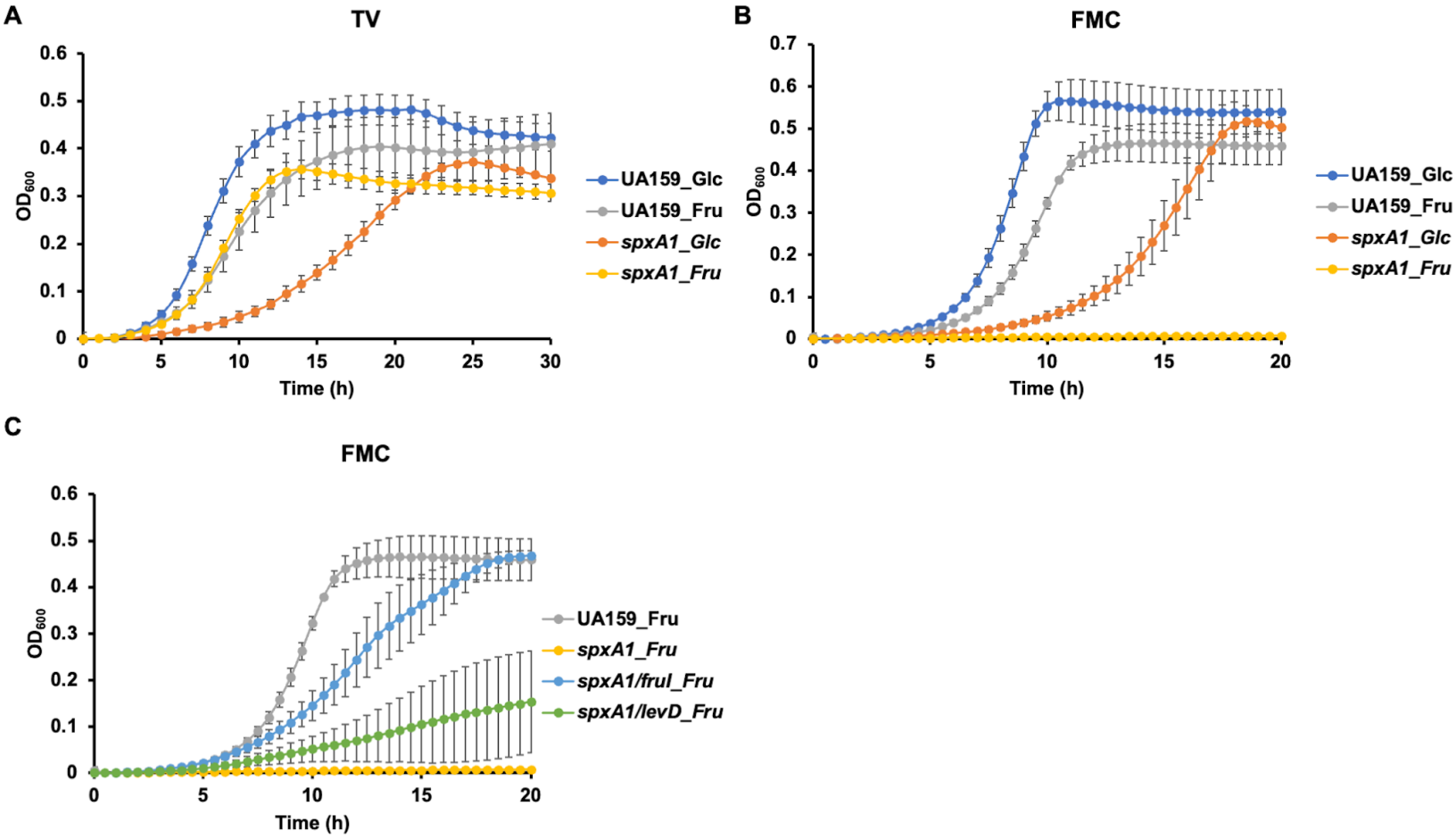
A
TV
OD600
Time (h)
UA159_Glc
UA159_Fru
spxA1_Glc
spxA1_Fru
B
FMC
OD600
Time (h)
UA159_Glc
UA159_Fru
spxA1_Glc
spxA1_Fru
C
FMC
OD600
Time (h)
UA159_Fru
spxA1_Fru
spxA1/fruI_Fru
spxA1/levD_Fru

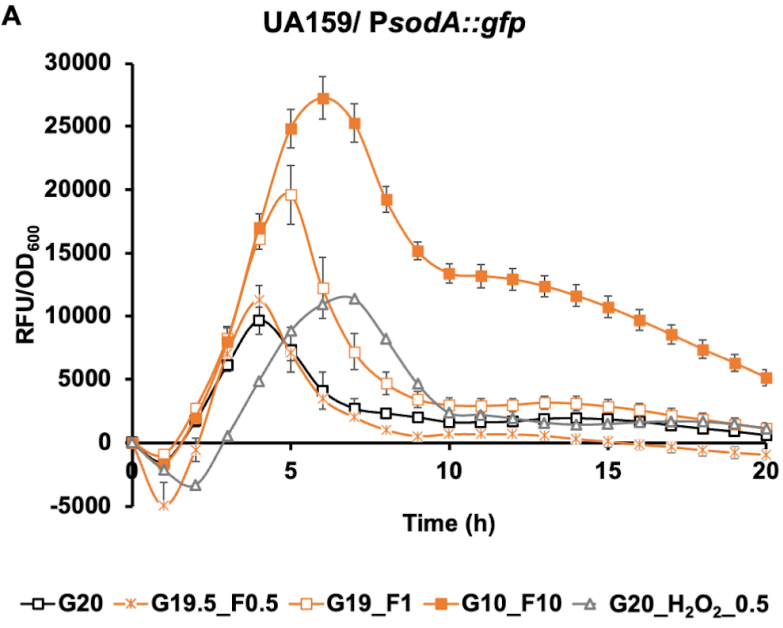
A
UA159/ PsodA::gfp
RFU/OD600
Time (h)
G20
G19.5_F0.5
G19_F1
G10_F10
G20_H2O2_0.5

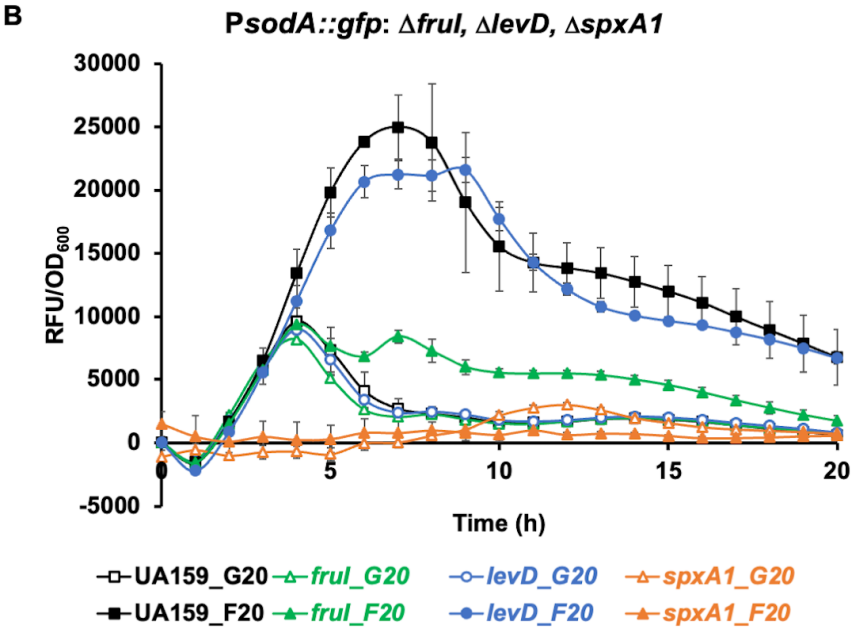
B
PsodA::gfp: ΔfruI, ΔlevD, ΔspxA1
RFU/OD600
Time (h)
UA159_G20
fruI_G20
levD_G20
spxA1_G20
UA159_F20
fruI_F20
levD_F20
spxA1_F20

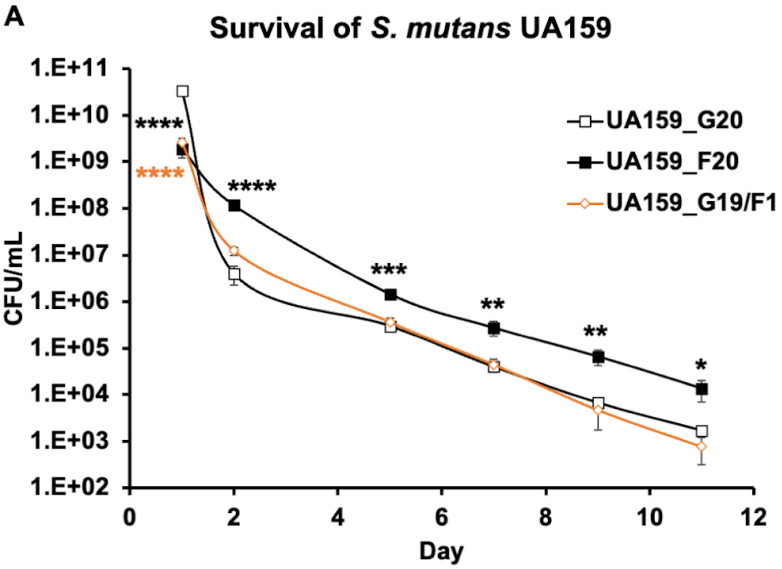
A
Survival of S. mutans UA159
1.E+11
1.E+10
1.E+09
1.E+08
1.E+07
1.E+06
1.E+05
1.E+04
1.E+03
1.E+02
CFU/mL
0
2
4
6
8
10
12
Day
UA159_G20
UA159_F20
UA159_G19/F1
****
****
****
***
**
**
*

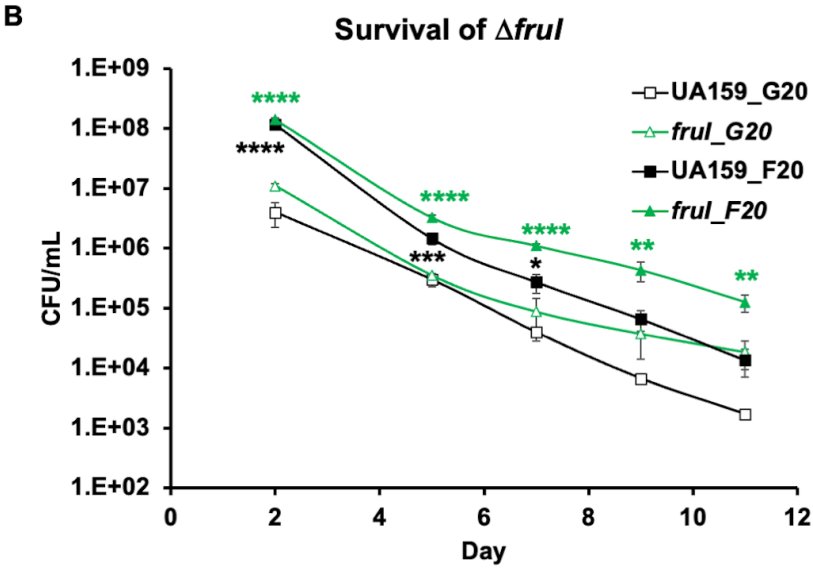
B
Survival of Δfrul
1.E+09
1.E+08
1.E+07
1.E+06
1.E+05
1.E+04
1.E+03
1.E+02
CFU/mL
0
2
4
6
8
10
12
Day
UA159_G20
frul_G20
UA159_F20
frul_F20
****
****
****
***
****
*
**
**

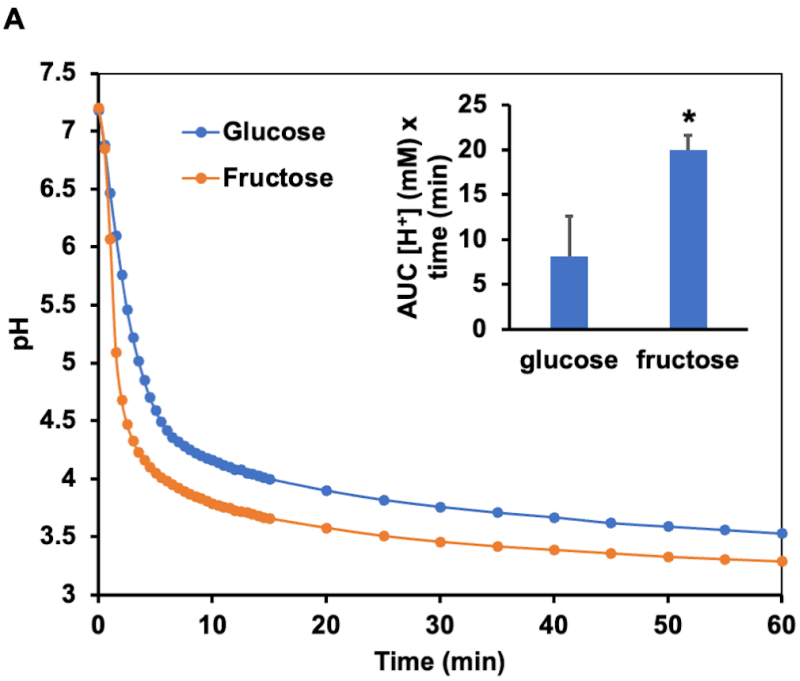
A
Glucose
Fructose
pH
Time (min)
AUC [H+] (mM) x time (min)
glucose
fructose
*

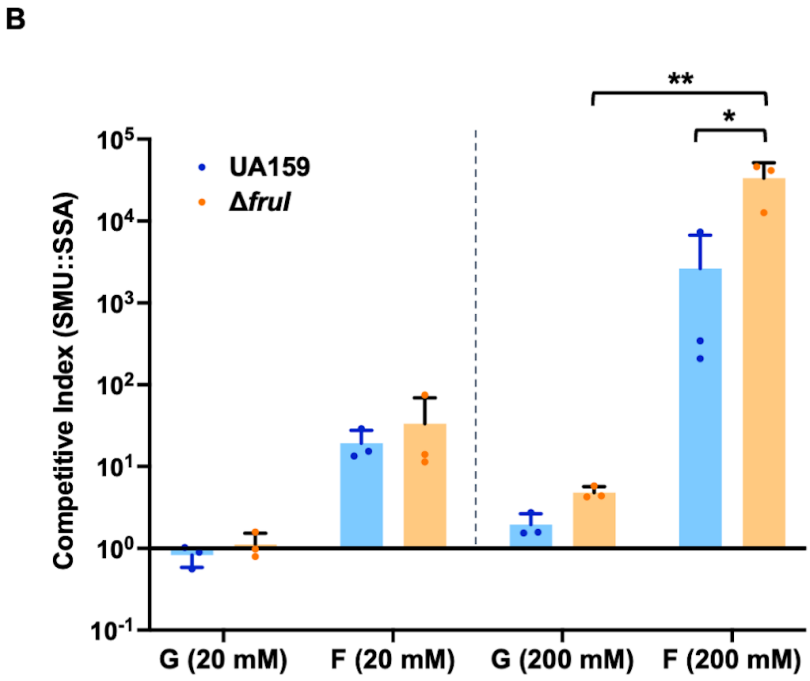
B
UA159
Δfrul
Competitive Index (SMU::SSA)
G (20 mM)
F (20 mM)
G (200 mM)
F (200 mM)
**
*

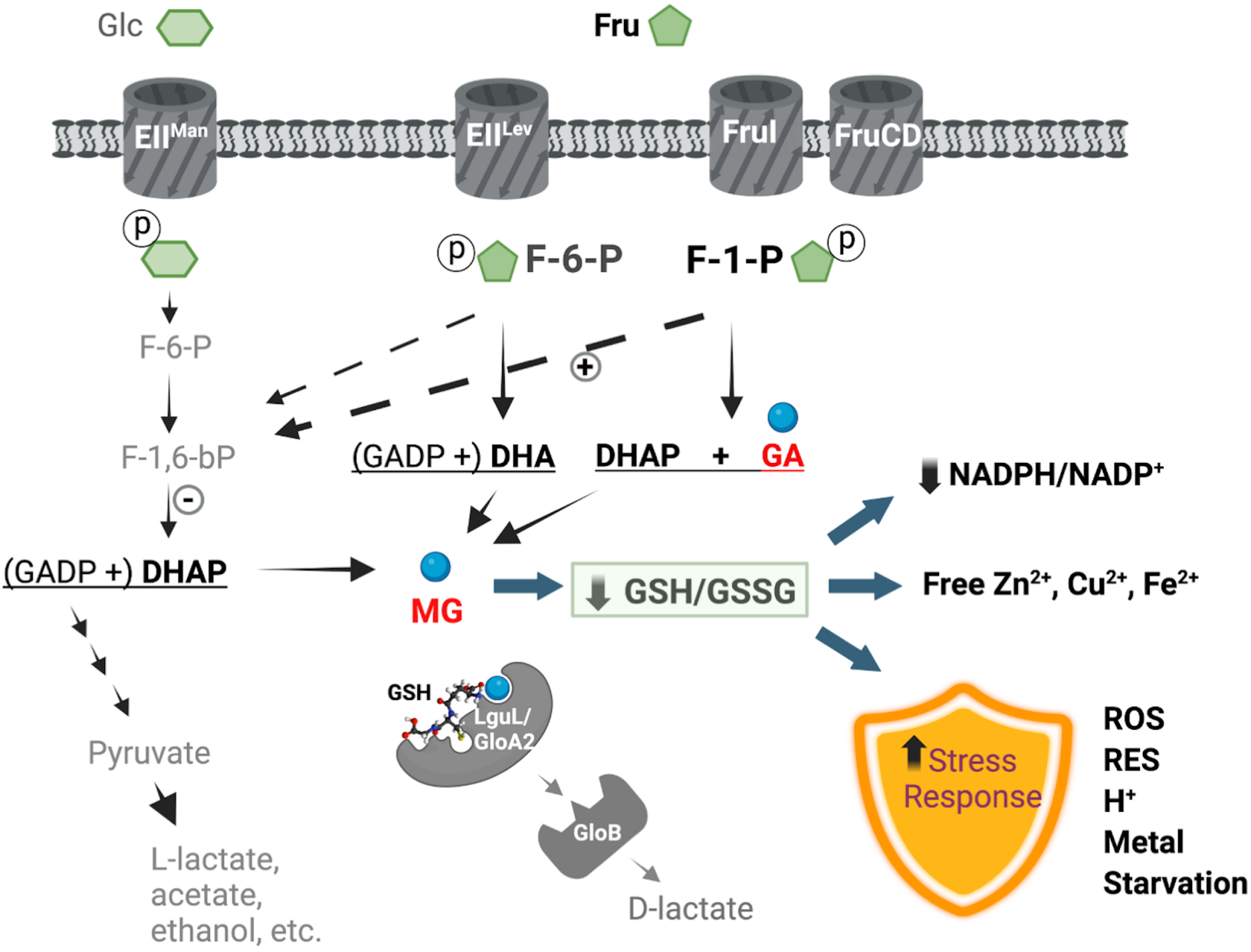
Glc
Fru
EIIMan
EIILev
FruI
FruCD
p
F-6-P
F-1-P
F-6-P
F-1,6-bP
(GADP +) DHA
DHAP + GA
NADPH/NADP+
(GADP +) DHAP
MG
GSH/GSSG
Free Zn2+, Cu2+, Fe2+
GSH
LguL/
GloA2
Stress
Response
ROS
RES
H+
Metal
Starvation
Pyruvate
GloB
L-lactate,
acetate,
ethanol, etc.
D-lactate